



DeepWind Deliverable

Grant Agreement number: 256769

Project title: Future Deep Sea Wind Turbine Technologies

Deliverable No.: D8.2

Deliverable title: Concept description & main components (R)

Deliverable status: closed

Name of lead beneficiary: DTU

Nature of deliverable: R

Dissemination level: PU

Due date from Annex 1: M44

Actual submission date: M48

Quality check approval by: Will be reviewed by Torben J. Larsen, DTU



The DeepWind concept, the controls & safety philosophy and the main 5 MW components

D8.2 Concept description & main components

Uwe Schmidt Paulsen, Helge Aagård Madsen, David Verelst, Per Hørlyk Nielsen, Troels Friis Pedersen Michael Borg, Luis Gonzales Seabra, Ewen Ritchie(AAU), Ole Svenstrup Petersen(DHI), Harald Svendsen(SINTEF), Petter Andreas Berthelsen(MARINTEK),

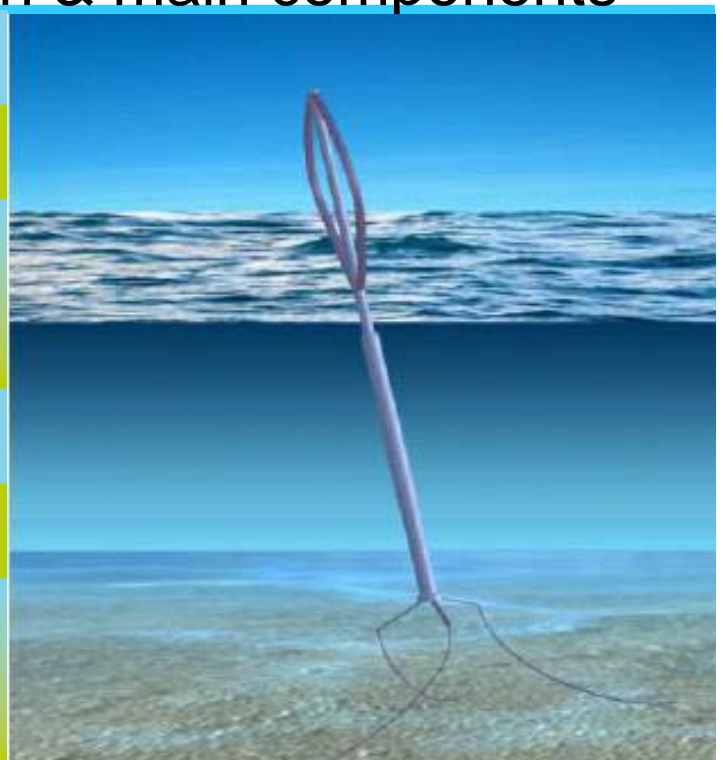
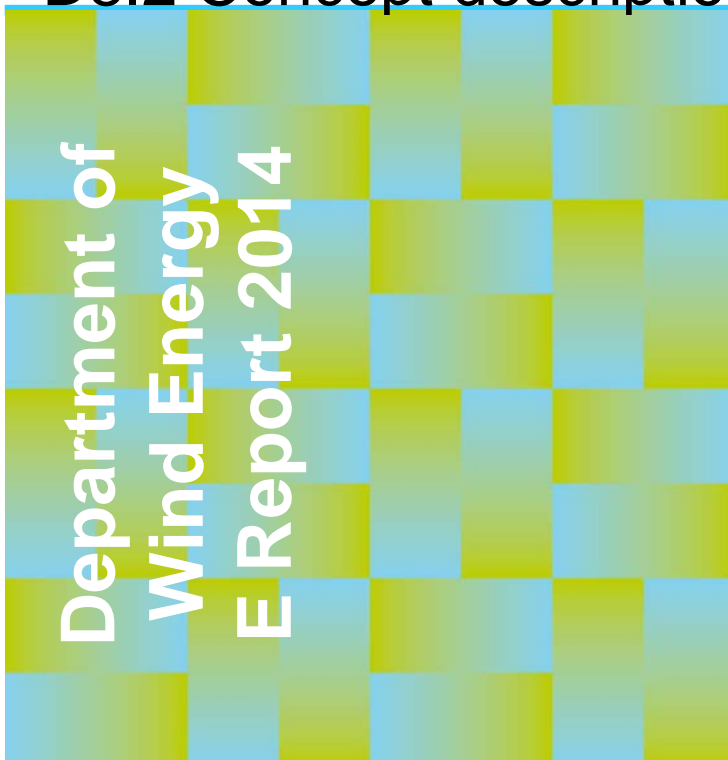
DTU Wind Energy-I-308(EN)

September 2014

Pp 59

The DeepWind concept, the controls & safety philosophy and the main 5 MW components

D8.2 Concept description & main components



Uwe Schmidt Paulsen, Helge Aagård Madsen, David Verelst, Per Hørlyk Nielsen, Troels Friis Pedersen Michael Borg, Luis Gonzales Seabra, Ewen Ritchie(AAU), Ole Svenstrup Petersen(DHI), Harald Svendsen(SINTEF), Petter Andreas Berthelsen(MARINTEK),

DTU Wind Energy-I-308(EN)

September 2014



Authors: Uwe Schmidt Paulsen, Helge Aagård Madsen, David Verelst, Per Hørlyk Nielsen, Troels Friis Pedersen Michael Borg, Luis Gonzales Seabra, Ewen Ritchie(AAU), Ole Svenstrup Petersen(DHI), Harald Svendsen(SINTEF), Petter Andreas Berthelsen(MARINTEK),

DTU Wind Energy-I-308(EN)
September 2014

Summary (max 2000 characters):

The report outlines the main components of the conceptual 5 MW design and in description of the parts a discussion of the results as they appear at project end. Reflections on installation, O&M and other variables in dealing with DeepWind are commented in the report. A comparison of the selected technical variables between the NREL 5 WM OC3 machine and the 5MW DeepWind conceptual design is carried out.

The work is a result of the contributions within the DeepWind project which is supported by the European Commission, Grant 256769 FP7 Energy 2010-Future emerging technologies, and by the DeepWind beneficiaries: DTU(DK), AAU(DK), TUDELFT(NL), TUTRENTO(I), DHI(DK), SINTEF(N), MARINTEK(N), MARIN(NL), NREL(USA), STATOIL(N), VESTAS(DK) and NENUPHAR(F).

Contract no.:
EC-256769

Project no.:
43057

Sponsorship:
EC-FP7

Front page:
DeepWind concepts

Pages: 59

Tables: 5

References: 13

Technical University of Denmark
Department of Wind Energy
Frederiksborgvej 399
Building 118
4000 Roskilde
Denmark
Phone 46775044

uwpa@dtu.dk
www.vindenergi.dtu.dk

Preface

The hypothesis of DeepWind is that this concept is developed specifically for offshore application and has potentials for better cost efficiency than existing offshore technology. Based on this hypothesis the objectives are:

- i. to explore the technologies needed for development of a new and simple floating offshore concept with a vertical axis rotor and a floating and rotating foundation,
- ii. to develop calculation and design tools for development and evaluation of very large wind turbines based on this concept and
- iii. evaluation of the overall concept with floating offshore horizontal axis wind turbines.

Upscaling of large rotors beyond 5MW has been expressed to have more cost potentials for vertical axis wind turbines than for horizontal axis wind turbines due to less influence of cyclic gravity loads. However, the technology behind the proposed concept presents extensive challenges needing explicit research, especially:

- dynamics of the system,
- pultruded blades with better material properties,
- sub-sea generator,
- mooring and torque absorption system, and
- torque, lift and drag on the rotating and floating haft foundation.

In order to be able in detail to evaluate the technologies behind the concept the project comprises:

1. numerical tools for prediction of energy production, dynamics, loads and fatigue,
2. tools for design and production of blades
3. tools for design of generator and controls,
4. design of mooring and torque absorption systems, and
5. knowledge of friction torque and lift and drag on rotating tube.

The technologies need verification, and in the project verification is made by:

6. proof-of concept testing of a small, kW sized technology demonstrator, partly under real conditions, partly under controlled laboratory conditions,
7. integration of all technologies in demonstration of the possibility of building a 5 MW wind turbine based on the concept, and an evaluation of the perspectives for the concept.

The results of WP01, WP02, WP03, WP04, WP05, and WP06 are integrated into a conceptual study of a new 5 MW design for comparison and evaluation against existing 5MW offshore horizontal axis wind turbine technology. Upscaling is explored against scaling trends from a 5 MW prototype towards a final 20 MW 'exercise'. Cost elements affecting the distribution of cost are surveyed, and effects with cost advantage potential are considered and the exercise accentuates differences of the concept compared to a 5 MW/ 20 MW offshore horizontal – axis turbine technologies. The results from the technical work packages are readdressed in terms of capitalised knowledge in the new technology field embracing compliance, safety and standards for offshore wind energy converters and the cost projections for upscaling are estimated by different levels of complexity. The ranges of application at site are specified for the final design layout calculations in WP01, Task 1.2. Applications of code, standards and regulations as well as decommissioning are surveyed into the calculations of the 5 MW design layout. This report describes site conditions which are relevant to apply for the present design.

Risø, August 2014

Uwe Schmidt Paulsen

Project manager and Co-ordinator of DeepWind

Content

Summary	8
1. INTRODUCTION.....	9
2. MAIN COMPONENTS DESCRIPTION.....	10
2.1 Overview of main components.....	10
2.2 Rotor and tower shaft.....	11
2.3 Floater and mooring system.....	14
2.4 Generator module	16
2.5 Controls.....	21
2.6 Layout of anchor points.....	29
2.7 Safety system	29
2.8 Assembly	31
2.9 Disassembly.....	32
2.10 O&M and decommissioning aspects.....	32
2.11 General remarks	34
3. Comparison of the 5 MW DeepWind with the NREL 5 MW OC3 platform	35
3.1 Power curve comparison.....	36
3.2 Annual Energy Production (AEP).....	39
3.3 Angles of inclination of the floater at WSL (tilt, roll and yaw).....	40
3.4 Position of the floater at WSL (sway, surge and heave).....	43
3.5 Forces of the floater at WSL	45
3.6 Bending moments of the floater at WSL.....	46
3.7 Bending moments from the blade root (bottom) to the blade root (top).....	49
References	53
Appendix A	Error! Bookmark not defined.
Acknowledgements	54

Summary

A specific survey of the concept, the controls & safety philosophy and the main 5 MW components is made, containing a description on the functions as well as components, the methods for assembling, transporting and installing the parts, and the methods intended for O&M. A comparison with existing 5 MW horizontal-axis turbines REPower 5M (NREL 5MW) is made.

1. INTRODUCTION

The aim of this report is to constitute a protocol manual to ensure harmonisation of offshore wind and wave simulation at facilities within the DeepWind project. Since this concept of a floating vertical-axis-wind turbine for offshore conditions is new to the wind sector and oil & gas industry, also the standards are not able to give answers to requirements that are described for horizontal-axis wind turbines. A specific survey of the concept, the controls & safety philosophy and the main 5 MW components is made, containing a description on the functions as well as components, the methods for assembling, transporting and installing the parts, and the methods intended for O&M. A comparison with existing 5 MW horizontal-axis turbines REPower 5M (NREL 5MW), mounted on a -OC3 spar is made. The report on the conditions and prerequisites for the DeepWind concept[1.] has to be consulted for additional information.

2. MAIN COMPONENTS DESCRIPTION

2.1 Overview of main components

In the description of the floating offshore wind turbine concept, the following components appear from a conceptual designs perspective:

- Rotor and tower shaft
- Floater
- Generator
- Controls
- Mooring system
- Safety system

In addition to the components, a system assuring the safe operation of the turbine during exceptional events, such as over speed or parking is suggested on a conceptual proposal.

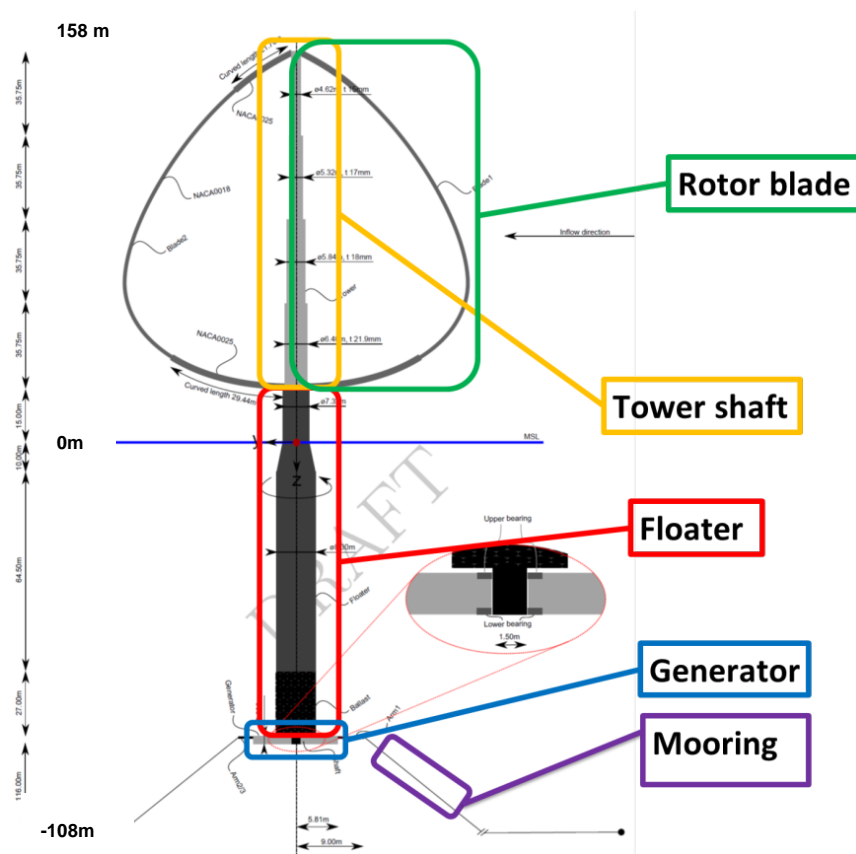


Figure 1 Overview diagram of 5 MW DeepWind conceptual design

The technical description for the rotor, floater, generator and mooring is provided in terms of the modelling characteristics presented in the detailed loads analysis report [2.]. In Table 1 main dimensions and operation data are given. In the following sections, each member of the structure (rotor, floater, generator, and electrical system, mooring line system and safety system) is described.

Table 1 5 MW DeepWind main geometric and operational data
Operational and Performance Data

Rated power	[MW]	5
Rated rotational speed	[rpm]	6
Rated wind speed	[m/s]	14
Cut in wind speed	[m/s]	4
Cut out wind speed	[m/s]	25
Geometry		
Rotor radius (R)	[m]	60.48
Rotor height (H)	[m]	143
Chord (c)	[m]	5
Solidity ($\sigma = Nc/R$)	[-]	0.1653
Swept Area	[m ²]	11996
Mooring line length	[m]	719.6

The annual energy production is estimated to 20 GWh and the rotor effectivity to exploit the wind is assumed to correspond to 190 Wm^{-2} . The wind turbine is stall controlled for wind speeds higher than 10 m/s and below this wind the rotor speed is variable.

2.2 Rotor and tower shaft

The rotor is made of pultruded sections. Three sections are used with a 25% airfoil section at each end where the flapwise blade bending moment is highest due to the own weight of the blade and then an 18% thick airfoil over the major, mid part of the rotor where a low drag is important.

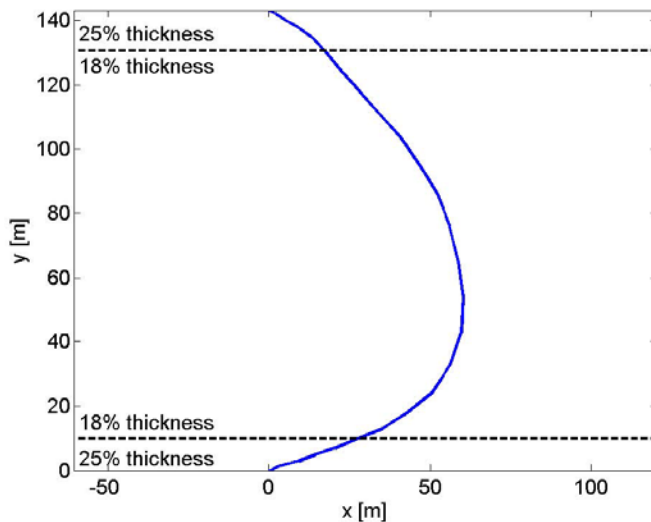


Figure 2 Rotor blade profile distribution

Each rotor blade is built of three sections; a section with 25% thick airfoils at each end at the attachment to the shaft where the flapwise moment are highest due to the eigen weight of the blades and then the main section on the central part of the rotor with an 18% airfoil where a relative thin airfoil with low drag is optimal.

Currently NACA symmetrical 4 digit profiles with thickness 25 and 18 % have been suggested in the conceptual study, but particularly a new generation of airfoils such as asymmetrical DU12W262 has been investigated in the Delft University wind tunnel for their ability to outperform NACA 0025 and 0018 airfoils and provide a more efficient section modulus index over the conventional design. This will be a task for future investigations as it was chosen to stay with the NACA0018 and NACA0025 airfoils for the present 5MW design studies due to the considerable experimental data to derive the airfoil characteristics to the present high Reynolds number around 10 mill.

The DU12W262 airfoil has a cross-section which is the result of an optimization for aerodynamic and structural performance. Selected from an initial population of airfoils through a genetic algorithm, the shape is evaluated via two objective functions (see D2.7 for details).

The sectionized parts of the rotor are manufactured with the techniques of pultrusion. Pultrusion is potentially a very efficient way to make very long constant chord GRP blades. A modelling tool has been developed for the pultrusion manufacturing method [5.] in the DeepWind project. The rotor form was derived in order to obtain low mean flapwise bending moments in the blades. This is illustrated in Figure 3 where the chosen rotor shape is shown in green in the left part of the figure. The flapwise bending moments in the right figure are seen to be low over the most part of the blade where an 18% airfoil was chosen and then at each end close to the shaft the moments are considerable higher and therefore a 25% section is used here. The chosen rotor shape has also the big advantage that the vertical position of the thrust force is lower than for the blue rotor shape and this reduces the cost of the floater

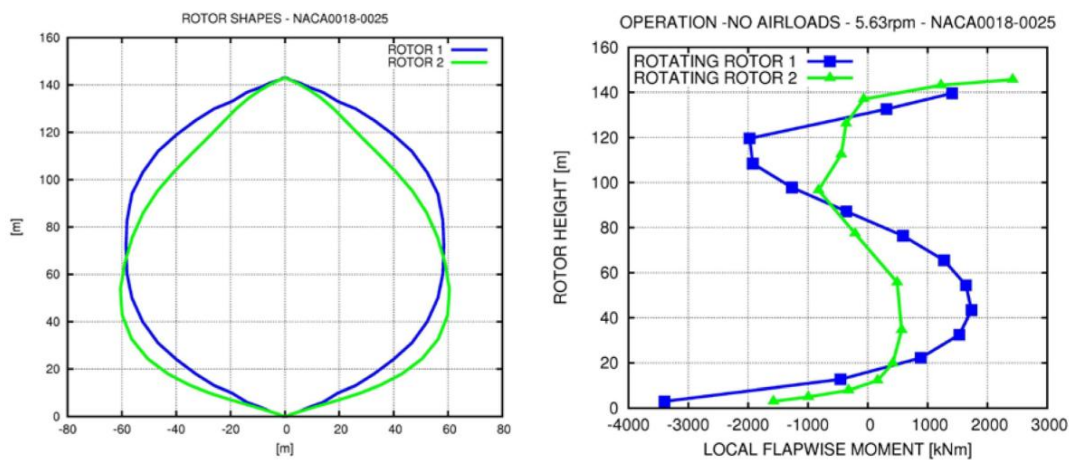


Figure 3 The development of the rotor shape to obtain low mean flapwise bending moments as illustrated by the rotor shape shown in green which was chosen for the final 5MW design.

Another main characteristic of the rotor design is that no supporting struts are used. It was considered to be of big importance to avoid struts for at least three reasons; 1) the horizontal struts and in particular the connections to the blades will create additional aerodynamic drag and thus also loss of power and; 2) The struts will create many more blade eigen frequencies which complicates the dynamic tailoring of the system and; 3) the joints between struts and blades will always be exposed to stress concentrations and fatigue.

The drawback of avoiding the struts is that the rotor blades become more flexible which means that the amplitude of the blade motions is bigger than for a blade with struts. This has been investigated in detail in WP1 in Task 1.3. One of the major results from this investigation is shown Figure 4 where contour plots of the standard deviation of the flapwise and edgewise motion of a blade section on the central part of the blade is shown. First it can be noticed that in general the deflection in flapwise direction is much less than in the edgewise direction. This is due to the tension in the blades caused by the centrifugal loading. This also indicates that for a VAWT blade the focus on blade stiffness should be on the edgewise stiffness as well as on the flapwise stiffness. On the contour plot to the right in Figure 4 it can be seen that in general the amplitudes in edgewise vibrations are much higher than in the flapwise direction. It is also appears from the plot that the operational range for the rpm should be selected carefully as there are many regions where the response is unacceptable high. The edgewise vibration issue is a quite normal characteristic for a stall controlled rotor and is likewise seen on stall controlled HAWT's.

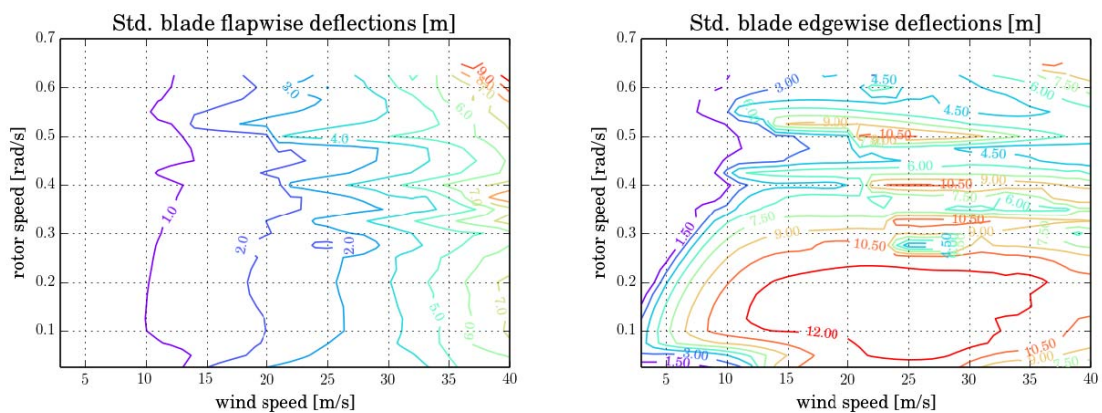


Figure 4 Contour plot of the standard deviation of vibration in the flapwise and edgewise direction of a blade section on the mid part of the rotor as function of rotor speed and wind speed. From D1.3.

Finally, the power and power coefficient curves are shown in Figure 5. The strong dependency of the maximum power on the rotor speed is characteristic for a stall regulated rotor and it could be built into the controller to reduce slightly the rotational speed in deep stall operation in order to reduce the loads.

The maximum power coefficient is seen to be close to 0.4 which is a typical value for a VAWT. It should also be noticed that the additional power production from variable speed operation seems not to be very big. In order to avoid the vibrational problems illustrated above a choice could be to run at almost constant rotational speed.

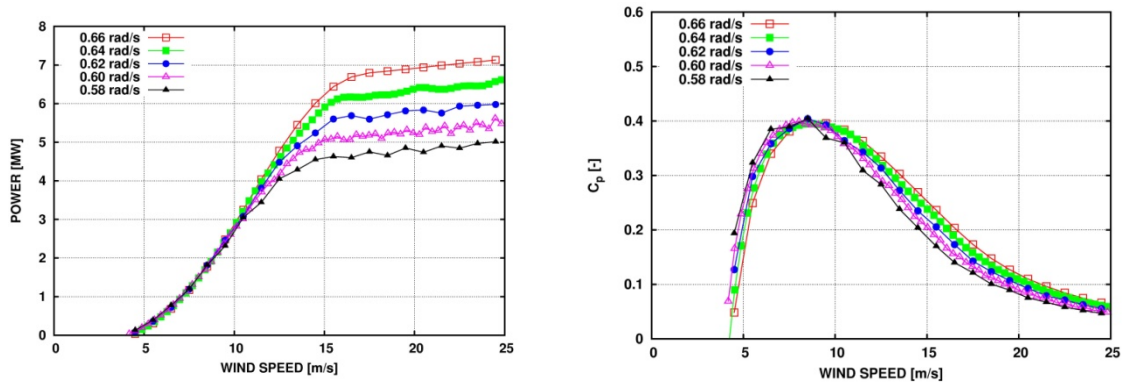


Figure 5 The mechanical power curves for the rotor for different rotational speed are shown in the left figure. To the right is the local power coefficient.

2.3 Floater and mooring system

The DeepWind project is based on a spar type floater. The spar is a deep draught vertical circular cylinder with buoyancy chambers at the upper part and a heavier section at the lower end for stabilization. The draught is usually deep enough to limit vertical wave forces such that the vertical motions of the spar buoy are rather small. A stable spar buoy design requires that the mass centre is located below the centre of buoyancy, ensuring that the floater stays upright with low roll and pitch motion. The upper part of the spar buoy is narrowed such that a small cross-sectional diameter is obtained in the wave zone, which limits the wave loads on the structure, and gives a vertical resonance period well above the energetic wave period range. The spar concept is commonly used in the offshore oil and gas industry as deep water production platforms, and it has shown to be a promising solution also for floating offshore wind turbines due to its favourable motion behaviour.

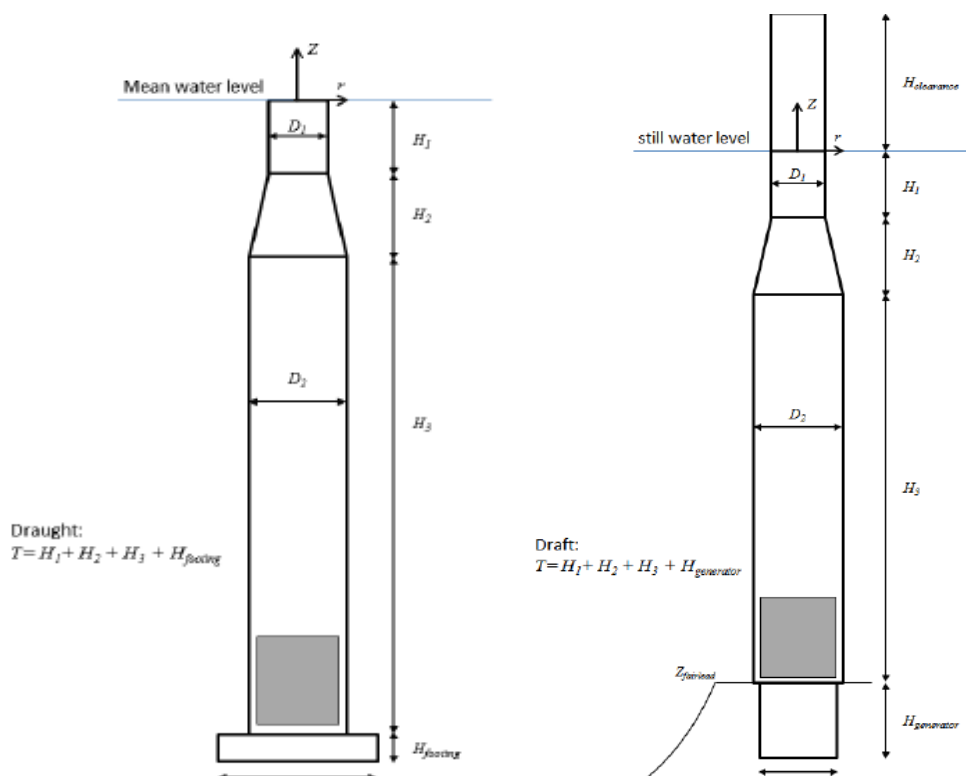


Figure 6 Left: 1st iteration design. Right: final floater design

The selection of hull shape and size depends on functional requirements, and the following basic design requirements should be considered for a floating wind turbine:

- Natural periods in heave and roll/pitch should be larger than the dominating wave periods to avoid resonant motion response.
- Sufficient buoyancy to carry specified payload and weight of the mooring system.
- Sufficient vertical stiffness for variable vertical load.
- Sufficient stiffness in roll and pitch to avoid excessive tilting of turbine axis due to environmental loads.
- Acceleration should be limited to avoid damage to machinery components.

Besides the environmental conditions, the dimension of the floater is mainly governed by the rotor design (both weight distribution and aerodynamic loads) and the specified payload (such as size and mass properties of the generator). Changes to the rotor or generator design will alter the shape and size of the spar hull.

Figure 6 illustrates the 1st iteration and final design of the floater, respectively. Various examples of the 1st iteration design floater are described in ref. [8.]. A revised version based on updated rotor and generator design is given in ref. [9.]. Steel is considered for the hull material, and the shape of the hull can be described as follows:

- A slender section near the water line.
- A transition section connecting the water line section to the main hull section.
- Upper main hull section is a voluminous section providing mainly buoyancy.
- Lower main hull section contains the solid ballast. The ballast material is un-compact, water saturated Olivine with density 2600 kg/m^3 .
- Bottom part which contains the generator.

Basic design requirements for mooring systems are:

- The extreme tension in the mooring lines should be less than the breaking strength (scaled by a safety factor)
- Sufficient fatigue life
- Sufficient horizontal stiffness to limit floater offset
- Sufficiently compliant (soft) system to avoid resonant motion induced by first order wave forces
- Adequate static horizontal pretension to provide sufficient yaw stiffness
- Redundancy

The mooring lines for the DeepWind concept must be designed so that it can withstand the large yaw moment from the rotating turbine. This requires a considerable stiffness in yaw.

The conceptual study [9.] considers two mooring system configuration:

- 3 line chain system. The lines are evenly spread at 120 deg.
- 6 line chain system. The lines are evenly spread at 60 deg.

The following concluding remarks were given in the study [9.]: “The conceptual design of a floating support structure and mooring system for the 5MW vertical axis DeepWind concept has been presented. The work has been carried out as the solution of an optimization problem where the optimization procedure tries to find a cheaper solution while satisfying a set of design requirements. However, it should be emphasized that the gradient search method tries to find improved solutions in the vicinity of the initial data, and due to the complex shape of the

constraint functions and inaccuracies of the numerical search algorithm the search may converge to local optima that are inferior to the best solution. On the other hand, the main focus of the study is the feasibility of the concept rather than finding an optimal solution. The results are intended to be used for further design iterations, including other sub-components, which will eventually result in a better integrated design. The mooring system design requires some special attention due to the large yaw moment caused by the rotating turbine. A minimum yaw stiffness is required in order to balance the wind induced yaw moment. The yaw stiffness is determined by the fairlead radius, the horizontal component of pretension and the number of mooring lines. To avoid too high loads on the mooring lines and fairlead connection, one possibility is to use a mooring configuration consisting of several mooring lines. The present results indicate that the cost for the additional lines for a 6-line configuration compared to a 3-line system is only marginal. The reason for this is that the 6 lines require smaller chain diameters due to less load per line. Low line tension is also positive with respect to fatigue. One important difference between the 3- and the 6-line system with respect to design is that the 6-line system has redundancy and will not pose any threat to neighbouring wind turbines in case of a line failure. DNV-OS-E301 recommends an increase in safety factors for non-redundant systems.”

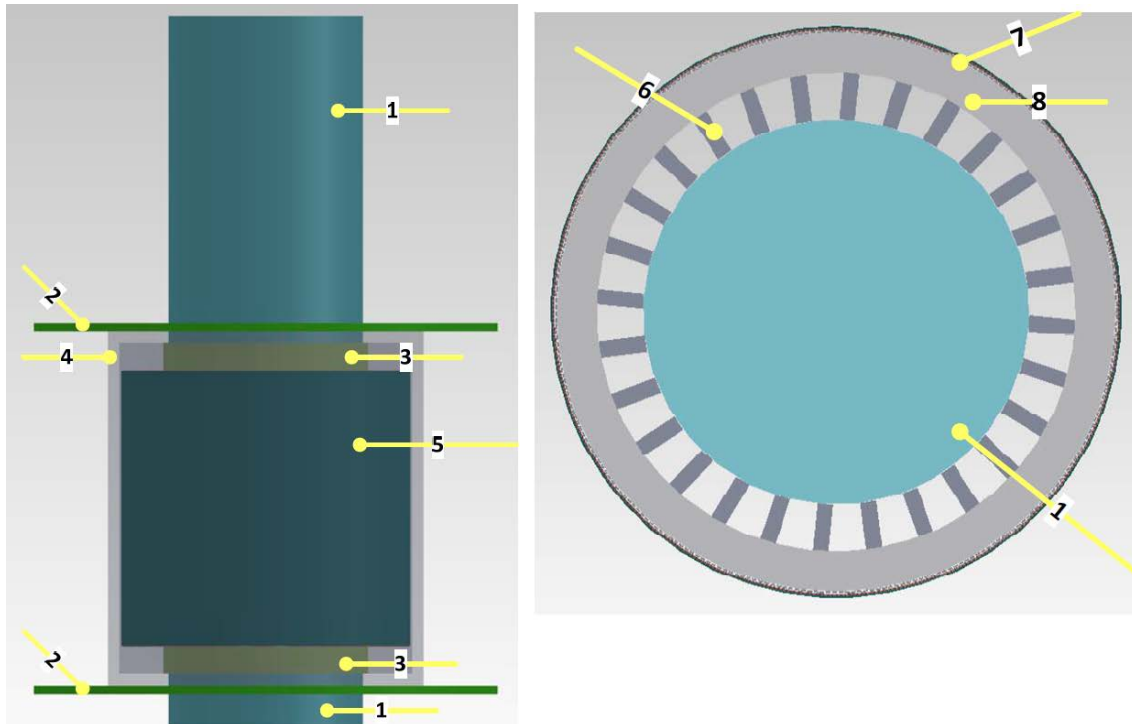
The conclusion points out that attention have to be put on the yaw stiffness, and on redundant safety of the mooring lines.

Presently the power loss due to friction from the rotating tube in water is simulated. In general it is within the rotational speed range 50-100 kW.

It should also be reiterated that the final design depends on input parameters such as rotor and generator design. Any changes or corrections to the input data (e.g. modifications to the rotor and generator design, changes to aerodynamic loads, etc.) may alter the present size and dimensions of the floater and mooring system.

2.4 Generator module

The generator module is made of the principal components sketched in Figure 7.



1-Floater	5-Generator
2-Axial Bearing	6-Support Spider Leg
3-Radial Bearing	7-airgap-active part of the generator
4-Generator Box	8- Rotor Core

Figure 7 Front -and top view section of generator and bearings[6.]

The tool for providing the generator design has provided a direct drive radial flux generator for wind turbine both for the 5 MW as well as the 20 MW concept designs. The main components of the 5MW DeepWind turbine electrical system are:

Electrical Generator

- 1 rotor (permanent magnets and iron lamination core)
- 1 stator (double layer concentrated windings-copper; iron lamination core)

Magnetic Bearings

- 1 radial (upper)-copper single layer concentrated windings + iron core
- 1 radial (lower)-copper single layer concentrated windings + iron core
- 2 x axial (upper and lower)-copper single layer concentrated windings + iron core

Structural Elements

- Spider connecting the generator rotor to the floater
- Generator box containing the electrical generator and 2 x radial magnetic bearings
- 4 x Bearing enclosures(2 for the axial and 2 for the radial bearings)

NOTE! : the solutions for the structural elements were only developed to a concept /proposed solution stage. With the specifications for the generator and bearings, the structural elements can be assessed. As future work, a thorough mechanical and chemical (corrosion) investigation can be carried out to obtain the final design of the structural elements listed previously.

The generator module is intended to provide a self-buoyant module, but with capacity for variable weight-buoyancy. The possible way to achieve this is shown in Figure 8 . Since the ballast tanks are intended to be used when installing and maintaining, cooling of the generator itself shall not be influenced under operation by this ballast tank.

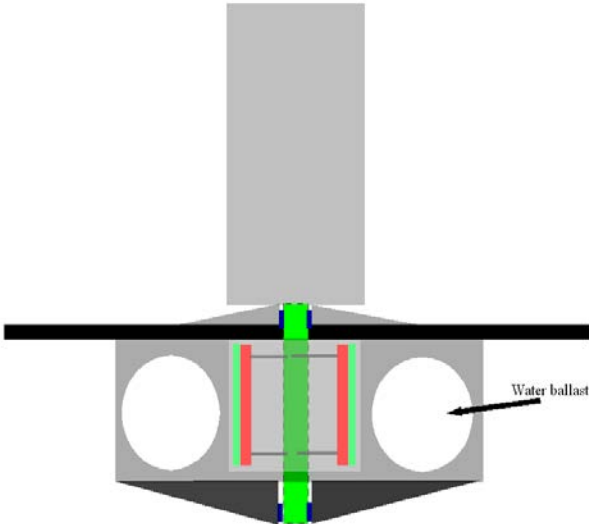


Figure 8 Artistic view of generator module, torque absorption and variable ballast section. The weight of the module can be variable by using pressurized air from a tank inside the floater, and through the hollow generator shaft out in the annular cavity holding water ballast and hence driving out parts of water, providing a net upward lift.©DTUWE

Table 2 DeepWind Power Electronics converters 5 MW system

5 MW 3 phase AC/AC power converter	1 stk		Main generator power converter
3*200 kW AC/DC phase power converter	1 stk	Requires sensors and controller	Upper radial bearing drive
3*112 kW AC/DC phase power converter	1 stk	Requires sensors and controller	Lower radial bearing drive
2*37.6 kW AC/DC phase power	2 stk	Requires sensors and controller	Axial bearing drive
Housing for all power converters	1 stk	Mounted on generator box or torque arms. Provided with air-conditioning to ensure dry air.	Contain and protect all power electronics

Connectors and cables	As required	Internal converters and generator/bearings	
Connector and cable (HVDC)	1 stk	Main power connection to grid	

The magnetic bearings are proposed because they can support the very large loads from the wind turbine/floater structure, even at standstill, and can be upscaled to accommodate larger shaft diameters and that in this way the point where the bearing is attached to the floater with respect to the distance from the sea water line is variable.

- How this can be optimized is an exercise for the next phase. An obvious positive effect is that the bearings and generator could be placed in or very close to the centre of gravity, with possible cost reduction potentials.

Currently the shaft is somewhat smaller, but with the potential to carry a commercial available generator module. The magnetic bearing requires active control, which demands power supply as seen from the specifications sheet. This power is not an indication of the average power consumption of the aggregates; the actual power loss is dependent on the actual loading of the shaft and the force required balancing these loads. In this sense the task for determining the power loss is integration and averaging of the power from these bearings, being a strong function of the instantaneous position of the shaft relative to the reference centre position, and the externally applied forces. These reactions are combinations of waves, currents and wind forces (thrust) (magnitude and direction relative to currents, which changes because of Coriolis forces with depth). The measured Coriolis effects on water laminae near the site have been introduced briefly in D8.1, where it is shown that a strong variation in magnitude and direction occurs over the entire floater draught. Some parts of the floater will be affected by a transverse force, and at deeper section the transverse force will be with different magnitude and in different direction. In conclusion a constant transverse force applied on the structure is very unlikely and pessimistic under real conditions. Coriolis effects are not implemented because of lack of data and complexity, and combined effects are discussed, but not calculated. These effects have to be investigated in the next phase for the actual site. We have assumed that the effects are functions much dominated by wind and have weighted the peak power for operating the magnetic bearings with a Rayleigh distribution for an average wind speed of 9.7 m/s. The bearing loss corresponds to 1%, or in average 50 kW bearings loss.

Another issue is with active control of the bearings, that in the event of no control-the shaft will suffer contact with the likely consequences of metallic rupture and failure of system. This is left as an engineering task to prevent this situation and provide a solution for rectification in the event of malfunction.

Maintenance

Due to the submarine location of the turbine and generator the level of maintenance must be minimized or preferably avoided.

Suggestions:

- Use system identification, approximations and predictions to determine full scale generator characteristic quantities on-line for diagnostic purposes
- Use monitoring and diagnostics to detect incipient faults and their progress towards unacceptable faults

- (i) Decide action for each fault type and level
 - (ii) Predefine the maintenance procedure for each expected fault.
- Provide the turbine and generator with built-in maintenance friendly features e.g. for a modular structure (proposed for the 20MW generator)-a controlled elevator that extracts and replaces a faulty coil with a healthy one with minimum assistance from the maintenance personnel.

The conversion of mechanical energy into electrical energy can be realized with the above module containing the generator and the bearings. Electronics known for being prone to regular replacements is suggested to be placed in a particular floating substation at sea level, as indicated in Figure 9.

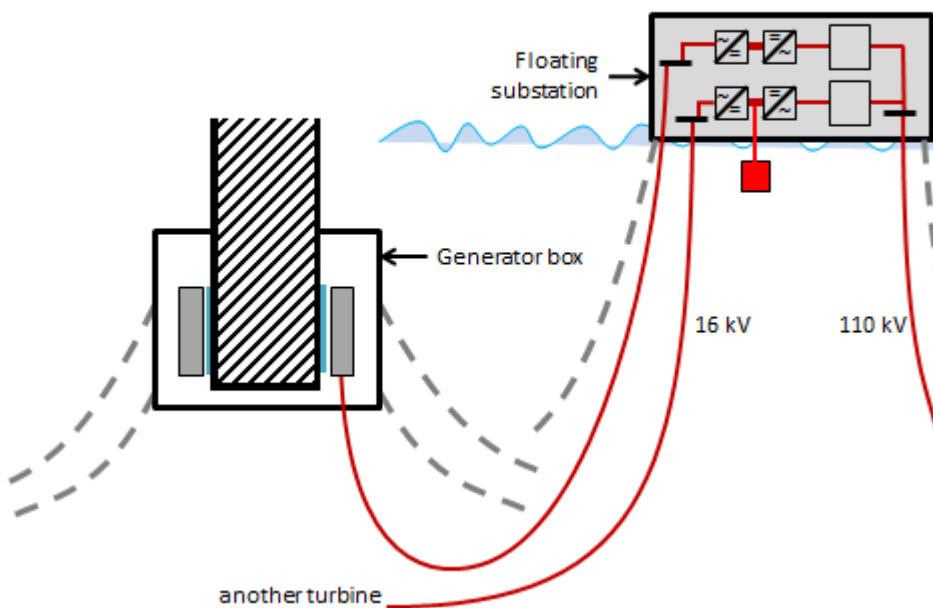


Figure 9 Sketch of Floating turbine and sea station arrangement

The system shown in Figure 9 offers obvious advantages over the systems shown in Figure 10, when unforeseen maintenance occurs in the event of breakdown of electronic components, requiring replacement so that the power system will go online.

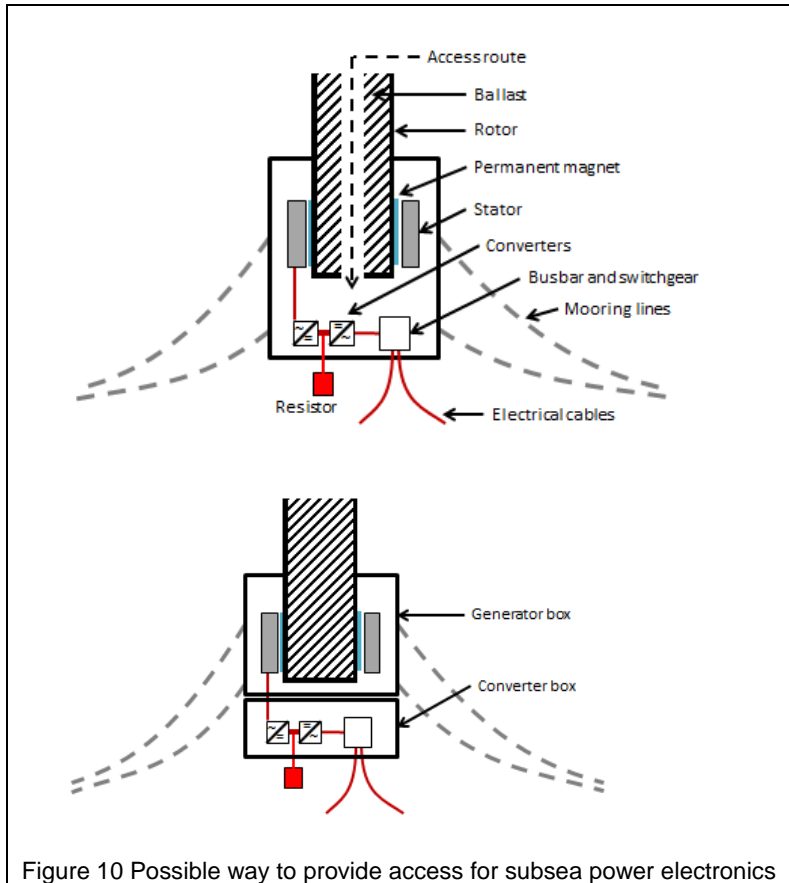


Figure 10 Possible way to provide access for subsea power electronics

2.5 Controls

The Work Package on Turbine Operational Control (WP4) focussed on the development of a baseline speed controller for the 5 MW DeepWind turbine, assuming a converter interface to the electrical grid. The output of the controller is a torque set-point, which determines the generator torque. The torque is adjusted to obtain the desired rotational speed. The main control objective is to ensure that the rotational speed follows a pre-defined operational schedule without unnecessary variations in either generator torque or the rotational speed itself. The main logic of the baseline controller is shown in Figure 11. It is a standard Proportional-Integral (PI) architecture with filters on the measured speed and torque input, and with gain scheduling on the proportional constant.

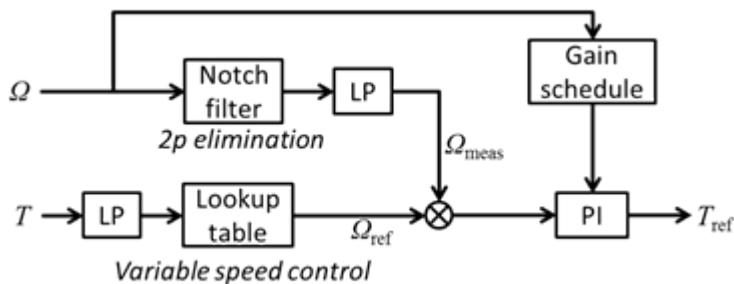


Figure 11 Overview of baseline controller logic

An important difference from control of horizontal axis turbines is the large variations in aerodynamic torque due to the non-alignment of the rotational axis and the wind direction. Technically the variations occur at the $n-p$ frequency, where n is the number of blades (e.g. for a 2-bladed VAWT, the variations are at $2p$). To isolate these large variations from the electrical system and the mooring system, a notch filter has been included. This filter eliminates $2p$ speed variations, effectively allowing the turbine to speed up and down in line with these torque variations and thus absorbing the power variations in its kinetic energy, allowing the generator torque and the mooring system torque to remain unaffected by the $2p$ aerodynamic torque variations. Simulation results show that this is indeed achieved to a very high degree with the notch filter.

Another important difference from conventional pitch-controlled horizontal axis turbines is that DeepWind is a stall-regulated turbine with no blade pitch degree of freedom. In this regard it has many similarities with horizontal-axis stall-regulated turbines. The main challenges related to this difference are firstly to understand and obtain a realistic description and simulation model for the aerodynamic behaviour in the stall regime in high winds, and secondly to achieve stable operation with rotational speed within pre-defined limits. The first challenge was tackled in two steps. First, a simplified approach was made by obtaining aerodynamic properties via a stream-tube blade element momentum approach. This was done for different wind speeds and rotational speeds to obtain coefficients of a Fourier approximation, taking into account $2p$ and $4p$ variations and including dynamic stall effects. These coefficients were then used in simulations via fast table look-up to give aerodynamic torque and thrust forces. This approximation gave good results when validated against more detailed descriptions. Towards the end of the project, this description was replaced by table look-up values obtained from HAWC2 simulations, without big changes in the results.

Compared to land-based vertical axis wind turbines, the most important difference from a control point of view is the fact that the stator part of the generator in the floating case is not fixed, but held in place by elastic mooring lines that means it has a rotational degree of freedom. In other words, the generator speed is not simply equal to the rotor speed, but the difference between the rotor and stator speeds. Since the stator/mooring system has low inertia compared to the tower/rotor, fast changes in the generator torque should be avoided since they tend to excite stator motion rather than changing the rotor speed.

Tuning of PI controller and low pass (LP) filter constants was performed through frequency analysis of a linearised version of the DeepWind model. Since all active control is via the generator torque, there is a trade-off between speed variations and torque variations: A speed deviation may be quickly corrected with a fast torque adjustment at the expense of an unwanted spike in generator torque. Too slow torque response, on the other hand, gives larger speed deviation. The parameters obtained through this tuning process gave well-behaved system in simplified model simulations, with generator torque variability that was characterised in deliverable D4.2.

Start-up and shut-down was investigated in some detail since they represent situations that put the system under severe strain, and because they are non-trivial, yet important operations. The aim was to implement start-up and shut-down strategies that would safely bring the system to idle operation in high or low wind, and be able to start the system again when conditions allow. An extended version of the controller, including the start/stop logic is illustrated in Figure 12. Filtered wind measurements are used instead of torque to determine turbine shut-down in high wind, and a fade-out of generator torque is suggested to ensure smooth transition from

operational to idle states. A storm control feature was included to limit the torque at high winds, whilst allowing the turbine to continue operation beyond 25 m/s.

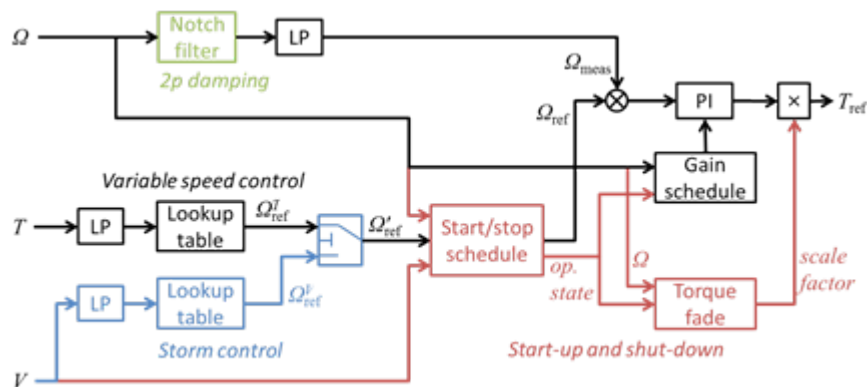


Figure 12 Control for start-up and shut-down

It is not sufficient to be able to operate the turbine in isolation; it must also be well-behaved when connected to the electrical grid. In this regard, it is essential that the system satisfies grid code requirements. With a full power converter connection to the grid, as illustrated in Figure 14, there is sufficient controllability to achieve this in principle. However, it is essential to ensure that the proposed control schemes for grid code compliance do not have severe negative effects on the mechanical parts. This was investigated and reported in deliverable D4.3, with particular emphasis on low voltage fault ride-through capability. It was verified that a control scheme based on a resistor in the DC link will work well, provided that such a resistor of sufficient size can be included in practice.

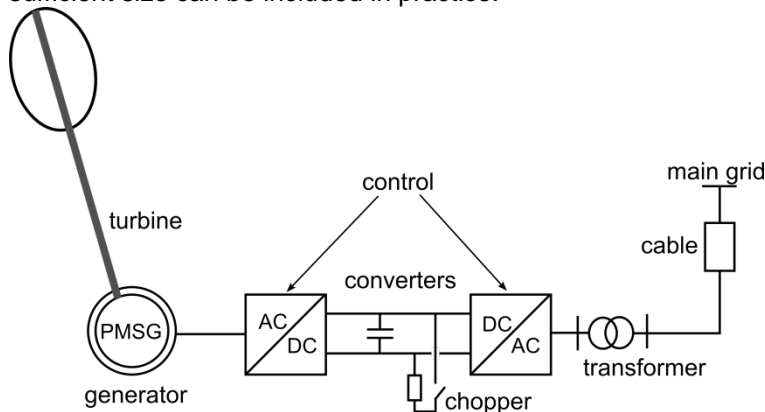


Figure 14 - Schematic of electrical system

The baseline controller was tested for a set of operating conditions both in a simplified model and in the detailed model, with promising results as noted above. However, it was not possible within the project to do a sufficiently comprehensive test in all relevant conditions using the detailed model. It is possible that additional unwanted effects, such as e.g. drivetrain oscillations may appear under some circumstances not yet considered. Such effects may be mitigated by adjustments to the controller tuning constants or additional control loops providing active damping. Significant uncertainties clearly remain regarding the controllability of the DeepWind system. However, the results from the investigations within this project give clear and positive indications that a reasonably standard control architecture can achieve a good performance.

Experiences on the control from time simulations in the full HAWC2 model

The above described control system was implemented in the full hydro-aero-elastic HAWC2 model of the 5MW Deepwind turbine. The full model now covers components according to the overview diagram in **Error! Reference source not found.** but as we will see below with some changes in model set-up had to be made to solve some observed dynamic instabilities. This process ideally requires more analyses of the complete system followed by adjustment of component designs and then new simulations on the complete system. This would be out of the limits of the project so what was done here were to make some few changes of component characteristics with the aim to get an overall insight into the loading on the components which are supposed to be representative for a final system after many iterations on simulations/design adjustments.

We will show the characteristics of the torque at the different turbine components, in order to have the basis for understanding the dynamic response of the system and in particular the dynamics in the drive train originating; i) from the rotor blades through the rotor shaft and ii) via the heavy floater to the iii) generator rotor and finally converted to the iv) reaction torque in the generator house connected via arms to the mooring lines,. The turbine components are shown schematically in **Error! Reference source not found.**

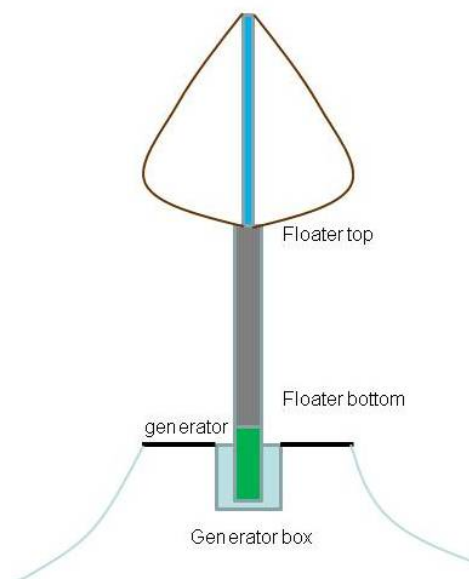


Figure 15 The main components important for the dynamics in the drive train system

The system dynamics will be characterized by showing results from a HAWC2 time simulation at 6m/s without turbulence and ss1. In the present case a fixed rotational speed is specified at the generator.

Operation at fixed rpm and without turbulence at 6m/s and ss1

As mentioned above in description of the control the torque input is highly unsteady as the blade torque is zero or negative at two positions over each rotor revolution as can be seen in the time

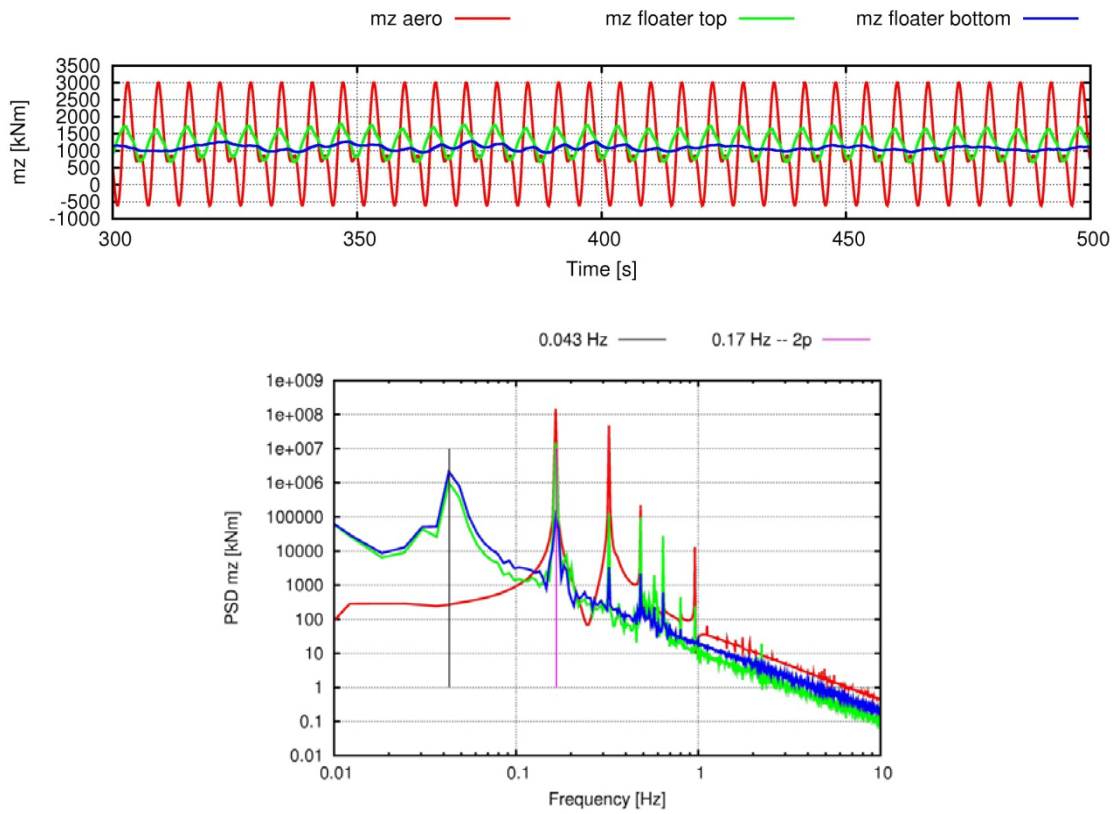


Figure 16 In the upper graph the torque is shown at different positions in the drive train. Below the PSD of the same signals are shown.

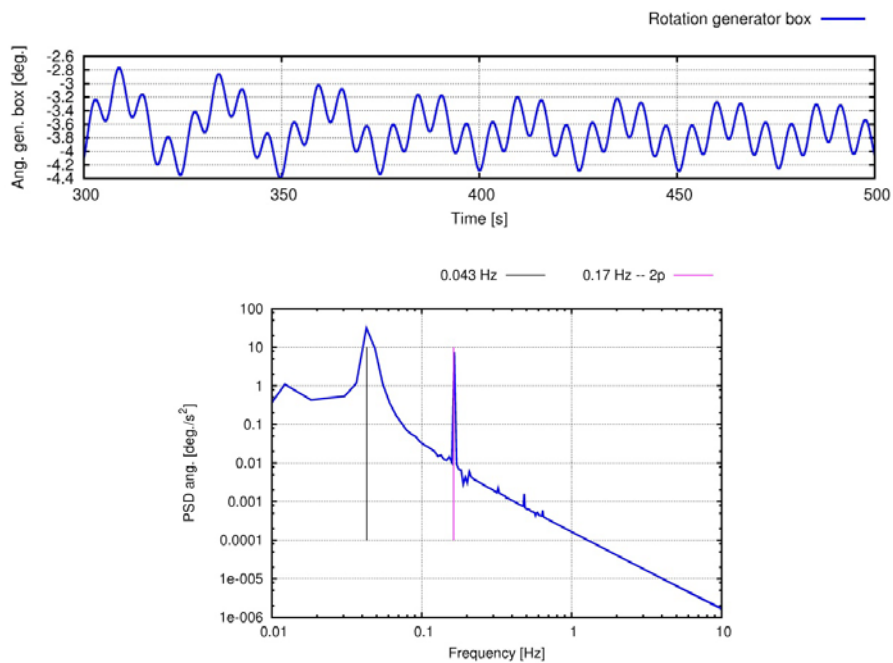


Figure 17 Upper graph shows the rotation of the generator box. The PSD of the same signal is shown in the lower graph.

trace in Figure 16. In the same graph is also shown the torque in the floater top and at the bottom of the floater and it is seen that the torque ripple here is reduced substantially. This is also clearly from the PSD of the same channels shown in the lower graph in Figure 16. The reason for this reduction of the aerodynamic torque ripple in spite of the constant speed is that the constant speed is relative to the generator box and as this is suspended softly by the mooring system, the generator box has a small angular rotation as seen in Figure 17. In the same figure the PSD of the angular rotation of the generator box shows that the frequency of the rotation is on $2p$ and on the eigen frequency of the rotation mode of the generator box and the yaw system, 0.043 Hz.

Operation with control at 6m/s and turbulence

Next we consider a case at 6m/s with turbulence and compare a simulation with control “on” and with a fixed rpm, respectively. As described above, one of the objectives of the control system is to dampen the strong $2p$ variations caused by the strong $2p$ content in the aerodynamic torque as was shown above. In the upper curve in Figure 18 it is seen that the torque curve with

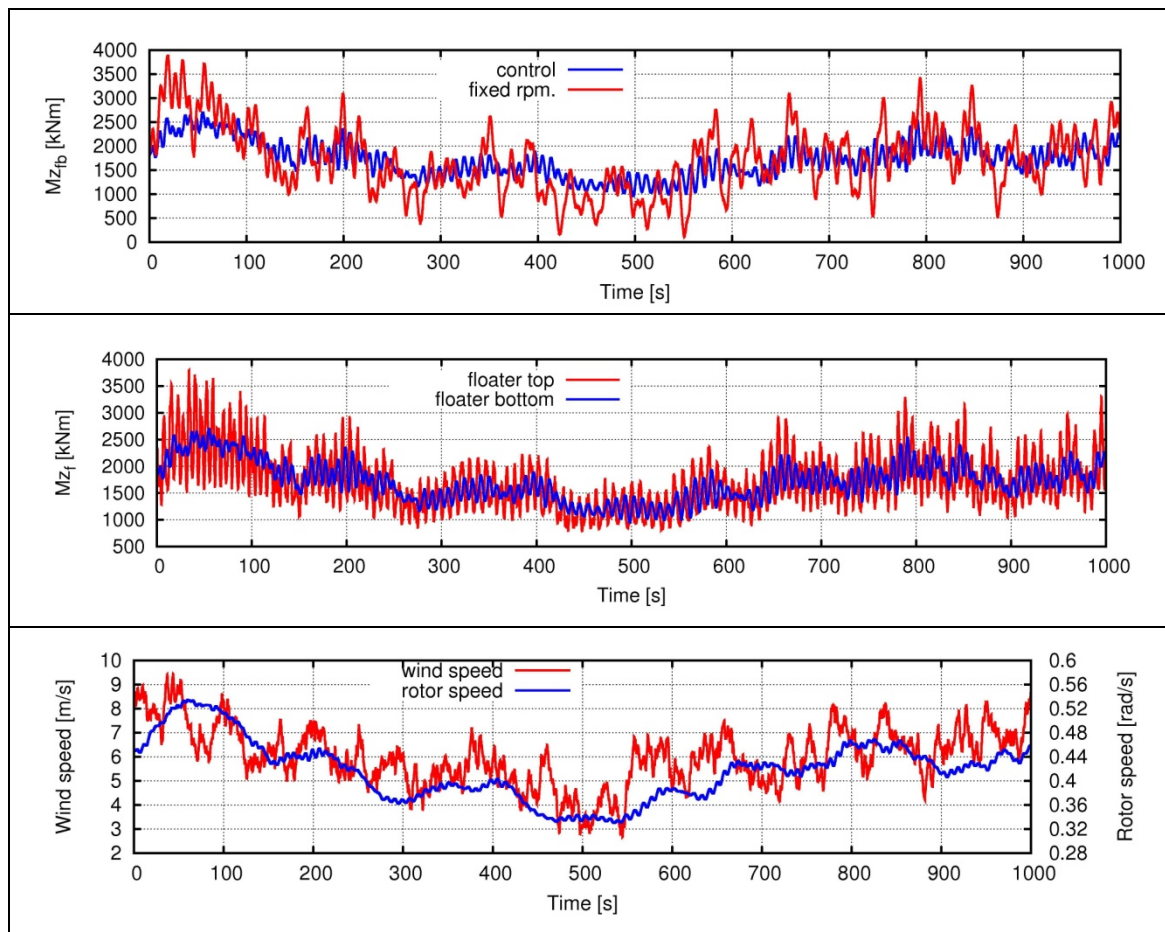


Figure 18 Upper graph shows the torque at the bottom of the floater with control and with fixed rpm, respectively. In the middle graph the torque at the top and bottom of the floater, respectively is compared for the case with control. Finally the rotational speed and the wind speed is shown in the lower graph.

the controller is much smoother than with the fixed rpm operation and this is also seen in the PSD of the same two curves in Figure 18. The mechanism of this smoothing or damping of the

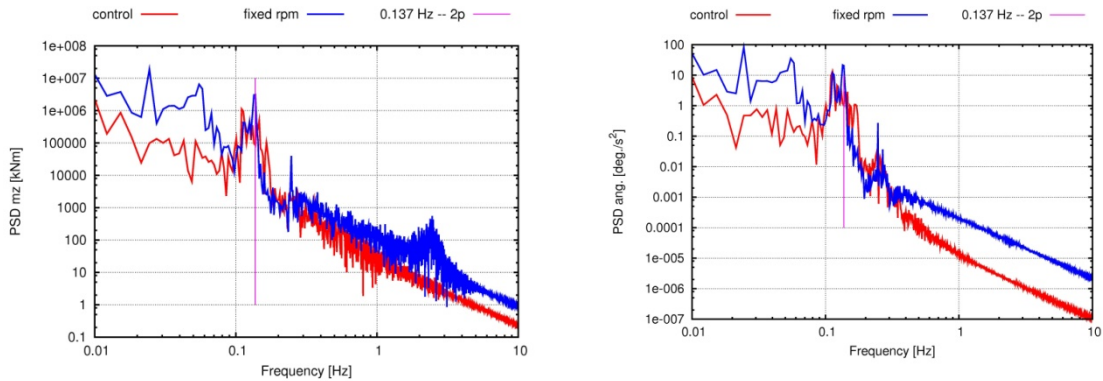


Figure 19 To the left is shown the PSD of the torque in the bottom of the floater for the control and fixed rpm case, respectively. To the right is shown the PSD of the angular rotation for the same two cases.

torque ripples is the combination of the small 2p variations in the rotational speed as shown in the middle graph of Figure 18 and the big inertia of the floater which means that the torque at the bottom of the floater is much less than at the top. Finally, the control also reduces the angular rotation of the generator box which means lower dynamic forces in the mooring lines. The reduced angular rotation is illustrated by the PSD of the angular rotation when compared with the PSD of the fixed rpm rotation, Figure 19.

Instabilities at high wind in the stall operation

Below we show the result of simulations at 14m/s without turbulence where an instability in the drive train system seems to occur. The blades in this case were considered stiff in order to avoid an edgewise instability in the blades. From the PSD of the torque in the floater Figure 20 bottom it can be seen that a large peak at 0.466 Hz (between 4 and 5p) occurs for the control case. Due to time constraints at the end of the project it was not possible to find the cause for this instability and thus not possible to alleviate it by changes in the control. The simulation with fixed rotational speed does not show the same instability but on the other hand there is significantly more energy in the frequency range around 0.055Hz which is the frequency of the yaw motion of the mooring system.

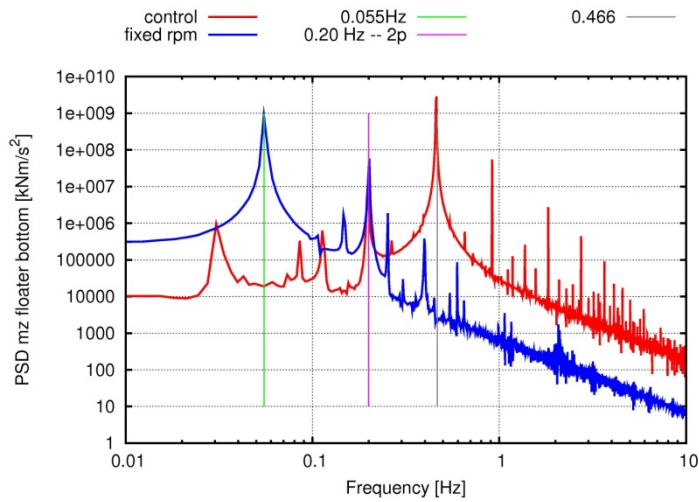


Figure 20 PSD of the torque at the floater bottom for a case at 14m/s with control and with fixed rotational speed, respectively.

Due to this instability it was decided to run the calculations used for comparison with the HAWT with fixed rpm. Further the simulations indicated that for the present 5MW design the tower was too soft with big translational amplitudes at the tower top. Therefore the simulations were run with a stiff tower and the stiffness of the blades were increased with a factor 2 in order to avoid an edgewise instability. The PSD of the torque in the floater for this configuration is shown below in Figure 21 with the biggest energy around 2p but also a distinct peak at 0.595 which relate to an edgewise frequency of the blades.

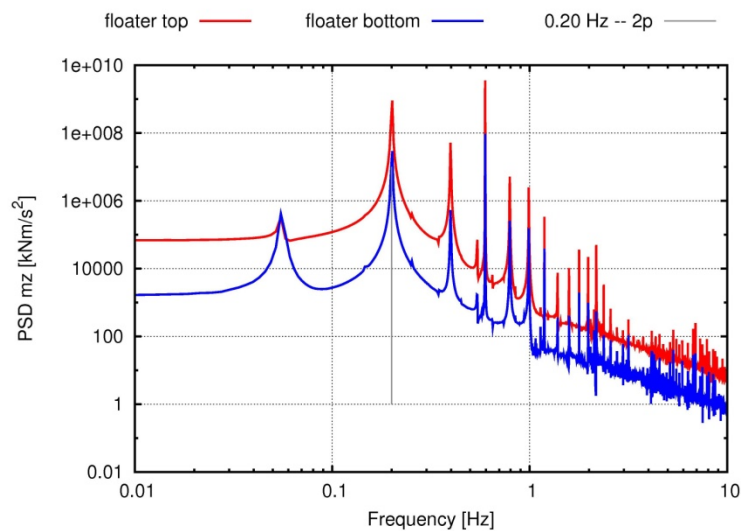


Figure 21 PSD of the torque in the top and bottom of the floater for a wind speed of 14m/s and fixed rotational speed.

2.6 Layout of anchor points

There are no detailed investigations providing analysis and results of optimized anchor point layout. The description of an a priori design is made in the paper describing the turbine floater and mooring system [8.] considering a single turbine only. However some considerations on shared anchor points have been provided in [4.]. A real, future application of the DeepWind floating turbine will be as part of a deep sea offshore wind farm. Additional questions then arise regarding the layout of the wind farm and the concepts for grid connection. These questions are basically the same for other types of offshore wind farms. However, a significant cost for floating wind turbines is related to the anchoring points. It is therefore beneficial for multiple turbines to share the same anchoring points, leading to a hexagonal turbine layout.

The mooring line and anchoring system is 10-30% of the 5 MW cost as shown in D8.3 . In order to make this more cost effective without any change in new materials, mooring- and anchoring technology, sharing of the anchor points can be obtained. A possible layout of a floating wind farm layout is shown in Figure 22 . With this system it is possible to cut 15% of anchor system on a sharing basis

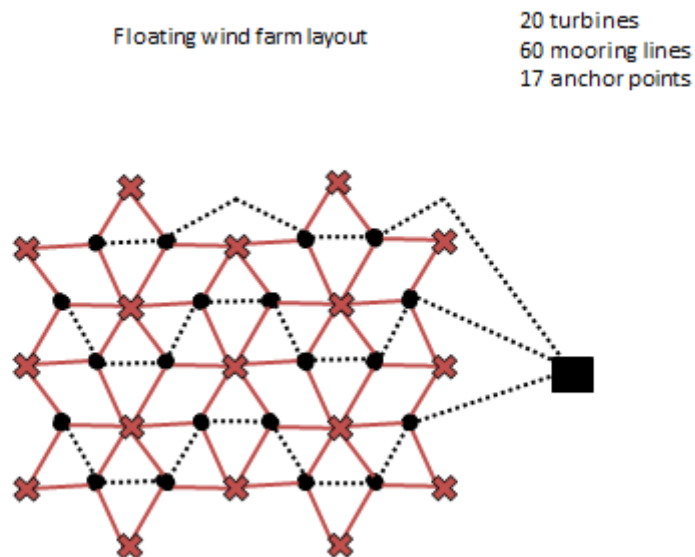


Figure 22 Wind farm layout, saving 33 anchor points out of 60.

2.7 Safety system

Within the project the consortium has investigated a safety systems approach and come up with a feasible and effective solution for both the safety system philosophy as well as a conceptual design for the 5MW machine. The solution shall also have the potential to be up-scaled to larger machines. The combination of the solutions is as it follows [8.]:

- 1) Torque Control for the generator used for power and speed regulation under normal conditions which is already designed and proposed through the Work Packages of Generator Design and Control Concept
- 2) Resistive Load Banks that cover braking requirements in case of loss of connection to the grid. These can be applied in two ways, each providing a different safety measure.

- a) When the grid connection is lost, but the machine side power electronics still functions, a resistive load can be connected in the DC link circuit of the power converter. This will provide controlled braking, as long as the floater is rotating.
 - b) When the grid connection is lost and the machine side converter is not functioning, the resistor bank can be connected directly to the generator terminals, either with a separate, dedicated control, or with no control. This will provide poorly controlled or uncontrolled braking as long as the floater is rotating.
- 3) A Parking Brake that could be a mechanical disc brake that can be activated during an emergency shutdown sequence that will be able to bring the rotor to zero rotational speed
 - 4) An additional safety system that would be used, in combination with the aforementioned systems or in case of a failure of the resistor load banks and torque control unit. It will be combined with a mechanical parking brake that will bring the rotor to stand still. However, even if the mechanical disc brake is under failure it is responsible to keep the wind turbine into safe rotational speeds under a freewheeling condition.

In the study [8.] proven airbrakes have been considered as an effective means to slow down the rpm of a wind turbine in overspeed conditions. Within the project outline there is an understanding that the use of water brakes will be around 1000 times more effective than airbrakes, and that the design of such an device is a matter of solving a dedicated engineering task. In the project we do not carry out these details as we are working on concept level. One promising safety system was developed by using the results obtained from the testing of the demonstrator in the fjord: the concept structure can be lowered in a controlled way to provide a potential efficient water brake system. The principle is explained in Figure 22.

Details are still open about stability of placing ballast at the top or, if combined with the power module, this can be improved. The blade base can be designed so that it can turn into a trapezoid shape closer to SWL and integrated into the blade and the tower.

The water brake system should be investigated further in details in dedicated experiments.

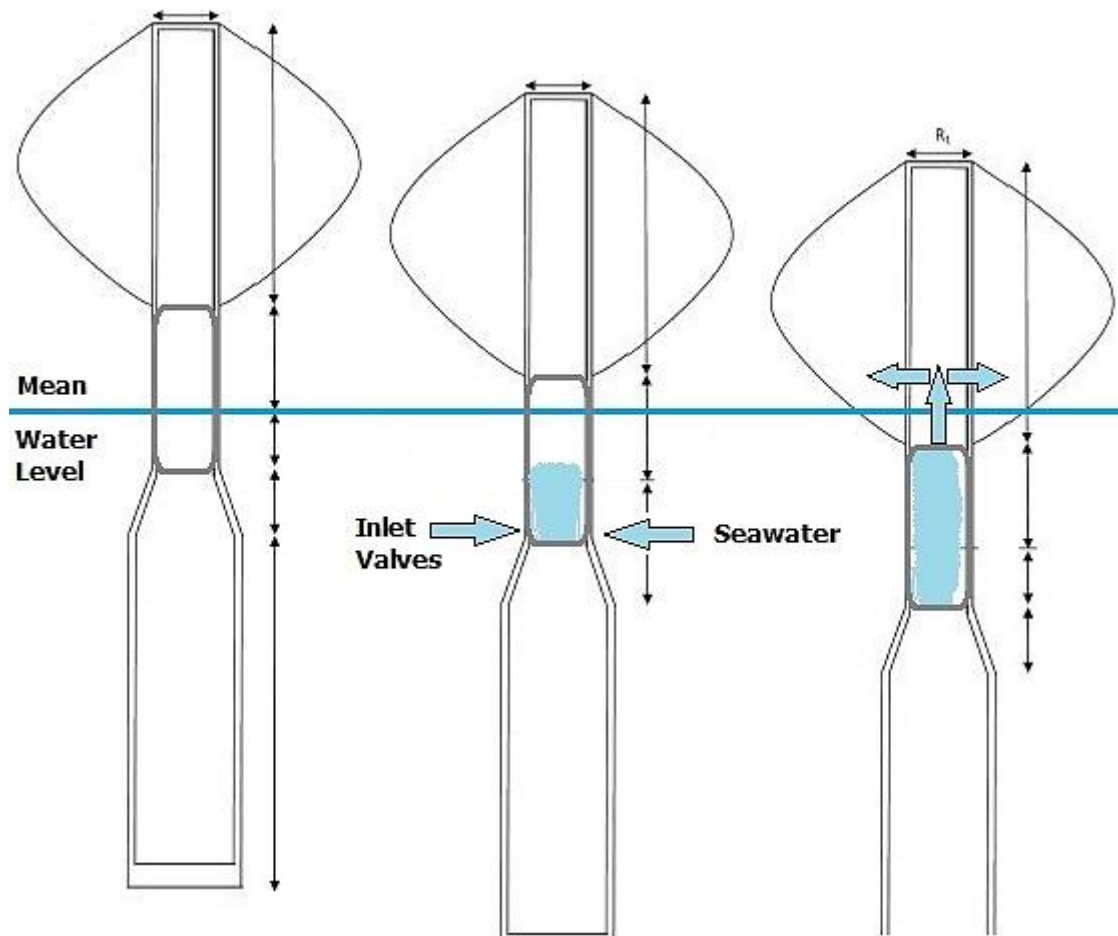


Figure 23 Sketch of the concept showing stages of the braking[8.]

2.8 Assembly

The following procedure is in its phase speculative and needs to be verified.

The assembly of the turbine is made prior in the port of where the turbine was built (e.g. shipyard). The system is towed to the site, either floating or on a barge. By means of the procedure of adding ballast in the ballast section, the turbine is gradually and in a controlled fashion positioned in place, as Figure 23 indicates.

The procedure does not need expensive cranes or vessels; two or three service ships may control the erection with the assistance of preinstalled lift bags for the capture of the mooring lines. For the underwater operation of securing the fairleads to buoys, underwater robotic submarines with monitoring capacity are needed. We assume that the generator module is equipped with an annular section that can be operated as a buoyant or ballast section, as indicated in Figure 8. The procedure for adding the water saturated olivine ballast in the ballast section has to be conducted. By opening a valve for the annular water ballast tanks and having compressed air as support for counteracting measures, the section can be descended in a controlled operation. Finally the mooring lines are adjusted by dragging the anchors in their final positions, in a coordinated action of removing the lifting bags connected to the fairleads.

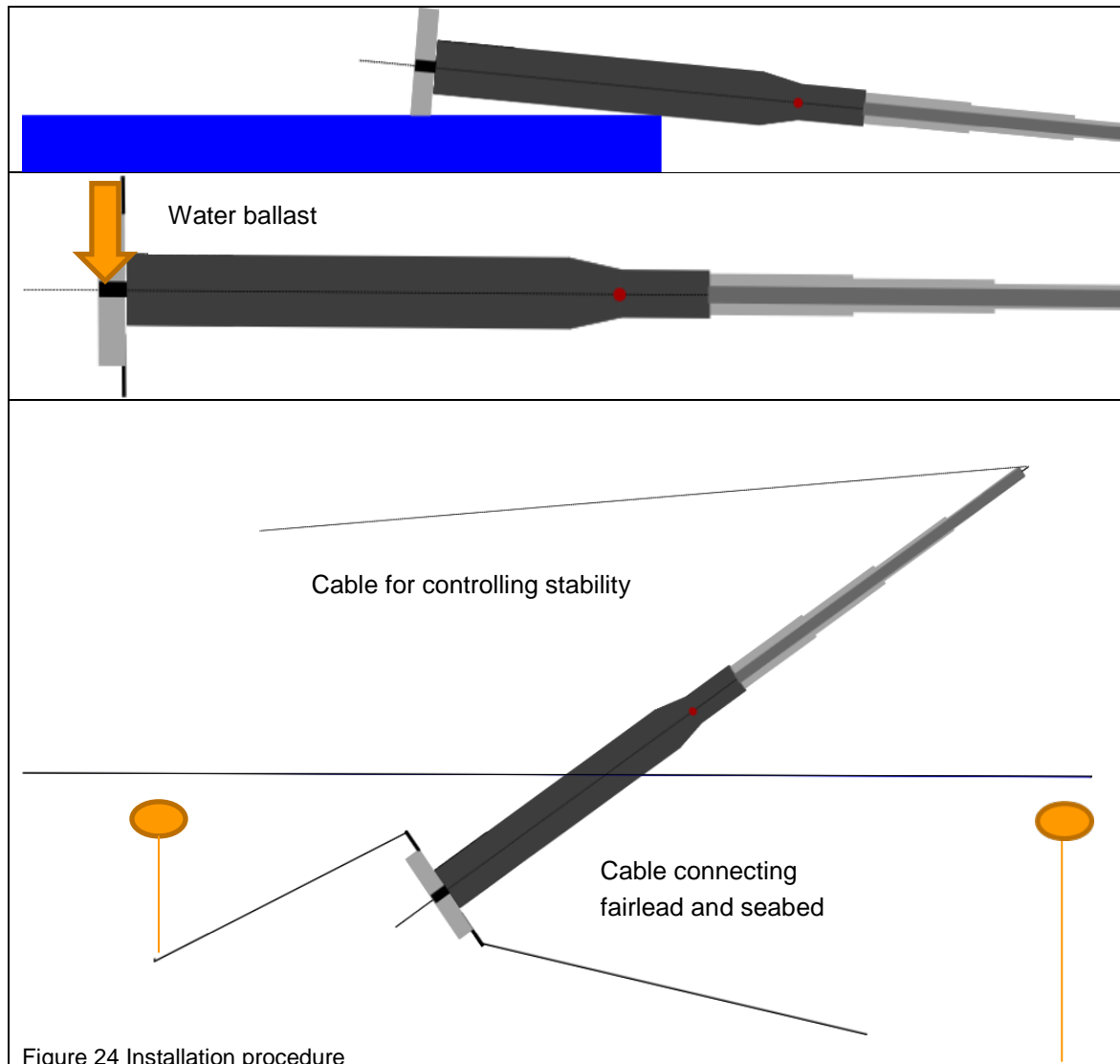


Figure 24 Installation procedure

2.9 Disassembly

The disassembly procedure is conducted in the reverse order than the assembly procedure. First the capture of the fairlead connections with lifting bags are carried out and secured. This requires possibly underwater robotic vehicles. The water ballast in the generator module is blown out and the slugging of the mooring lines is done.

2.10 O&M and decommissioning aspects

Marine growth and implications for O&M

The maintenance of the floater is intended to be carried out by means of cleaning the floater for marine growth. The marine growth even under the temperature ranges given, will provide an additional power loss due to friction [11.], from an additional layer of δ as: $(1+(r_2/r_1)^4)C_{f2}/C_{f1}h_2/h_1$ ($1/(1+h_2/h_1)$), which in this case will be approximately $4(r_2/r_1) \approx 4(1+\delta)$.

Underwater remote operated vehicles (ROVs), equipped with equipment delivering high pressure water jets can remove the marine growth from the floater. Because the growth can be variable with water temperature, sun exposure, saline - and other conditions and vary with depth down to 40 metres (Norwegian Sea), it can also be done by divers. However, to provide simple and labour efficient routines, these small underwater service stations are recommended

because of their potential to operate extensively over several hours, which is not the case for divers. They need strict diving times and contingency equipment and measures (rescue and assistance, pressure chamber, communications with land) for personal safety reasons.

Marine growth and implications for O&M at other sites than Karmøy

Marine growth on submerged structural components and other parts of a structure can have a significant influence on the hydrodynamic actions to which the structure is exposed, in particular the DeepWind concept.

The influence of marine growth on hydrodynamic actions is due to increased dimensions and increased drag coefficients due to roughness, as well as to the increased mass and its influence on dynamic response and the associated mass inertial forces. Where sufficient information is available, the loading coefficients may be selected based on the nature of the marine growth. Different types of marine growth (see Figure 24) occur at different water depths and in different parts of the region. For sites in subtropical and tropical regions, like in the seas of the East Asian region, growth is reported as much as 500mm [12.]. An anti-fouling coating can delay marine growth, but significant fouling is likely within 2 years to 4 years. For the particular site of the Hywind installation, a marine layer is reported in the order of 60 -100 mm (59° N to 72° N) [12.]

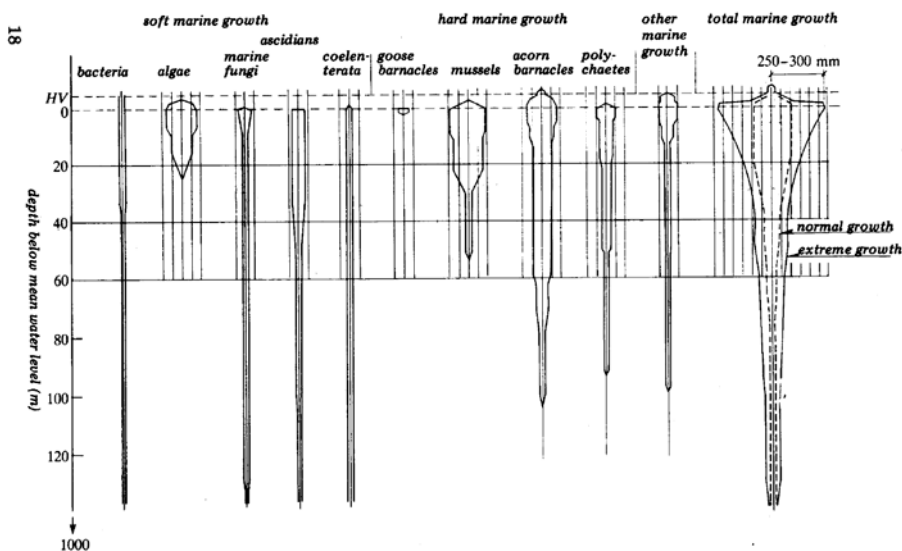


Figure 25 Distribution with depth of marine growth

It is suggested to use ROVs with accessory and dedicated equipment which might be able to clean of algae from the rotating spar and do other simple works. Because algae are most aggregate on the floater down to 40/60 m depth, it seems also plausible to use divers. Diving operators are frequently used in offshore and marine sector for different sorts of works down to 400m depths. However, we have no information about the assumptions and costing of diving operations; from a business solution perspective it makes sense to choose the unmanned (remote controlled) robotic vehicle as the instrument for doing the tasks. It will require a trained person (with assistant and a small lifting aid) to inaugurate the vehicle and to control the operations from the mother vessel (no much space required) without human hazard potential.

Decommissioning

Some material may have strange impacts on how to treat them after the turbine is dismantled. Floater material such as concrete (fibre composite concrete or similar) needs special treatment and procedures.

2.11 General remarks

Although not being able to provide details of costing and procedures involved in this phase of the concept, sum guideline can be applied:

- Costly installation vessels are not foreseen. Instead ordinary types of vessels (barge, towing vessel, tug boat) equipped with standard equipment such as lifting cranes and anchor winches are expected to be used, which in terms of extend looks similar to small marine operations.
- During maintenance the crew can live on a floating hotel for people assisting in the maintenance operations (standard in marine sector)
- Lifting bags, remote operated vehicles (ROVs), and non-specialised assistants are forming the cornerstone of a team for installation, and maintenance purposes
- ROV is a potential sound technology for assisting DeepWind in installation, maintenance (particular cleaning of marine growth) and when the power plant has to be decommissioned. New technology allowing for remote control of the tasks being done underwater from a single crew member above sea level will cut safety risk to a bare minimum in terms of human accidents that can happen with diver assisted works
- Operation of the demonstrator showed heavy wear of the metalling materials due to partly presence of barnacles (hard shell) and galvanic corrosion (GC). Protection methods such as painting, sacrifice cathodes (zink) or applying a current to oppose GC are proven technologies that helped. GC will be an event for regular maintenance, very well known in marine sector maintenance.
- The procedures for installing the turbine, maintenance and dismantling are important to validate in experiment.
- It should be investigated if marine life can prospect from sinking the structures to form living grounds for underwater habitats.

The above considerations are based on that presence of mammals and sea life are not influenced negatively by the presence of DeepWind during installation, operation and maintenance. Recent observations on bridge pillars and on sunken ships confirm this effect of placing man-made structures on the seafloor. Also, recent observations of sunken ships at depths of 300-3000m have shown marine life activity.

3. Comparison of the 5 MW DeepWind with the NREL 5 MW OC3 platform

In this section a quantitative comparison of different parameters under normal operation conditions between the DeepWind (FVAWT 5MW) and the NREL 5MW Floating Spar Buoy (reference model used in the Offshore Code Comparison Collaborative - OC3) was performed.

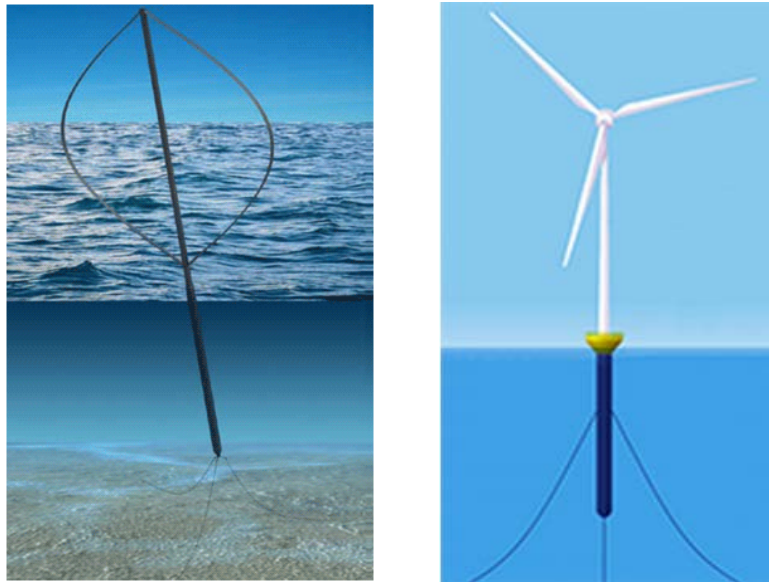


Figure 26 DeepWind 5MW FVAWT (left) and NREL 5MW FVAWT (right)

Illustration by: DTU Risø Campus and www.hawc2.dk

Some brief operational parameters are described in the table below that are relevant to the operational comparison:

	FVAWT DeepWind	FVAWT NREL
Rated power [MW]	5	5
Rated rotational speed [rpm]	5.95	12.1
Rated rotational speed [rad/s]	0.62	1.27
Rated wind speed [m/s]	14	12
Cut in wind speed [m/s]	4	4
Cut out wind speed [m/s]	25	25
Rotor radius [m]	60.49	63
Rotor height / Hub height [m]	143	79.6
Max Blade chord [m]	5.000	4.652
Swept area [m²]	11996	12469

Table 3 FVAWT and FVAWT Operational parameters

3.1 Power curve comparison

The Power curves of both wind turbine models were calculated using HAWC2 (v11.8) under simulations of 1000s for each wind speed (range from 4 to 24 m/s, with a 2m/s step) under wind conditions of deterministic and turbulent inflow respectively. For the hydrodynamic model implemented in HAWC2, three sea states of regular waves were used including the current effect (waves and current same direction of the wind) as described in the Table below:

	H_s [m]	T_s [s]	Current [m/s]
Sea State 1	4	9	0.35 for V ₀ < 14 m/s, 0.7 for V ₀ > 14 m/s
Sea State 2	9	13.2	0.35 for V ₀ < 14 m/s, 0.7 for V ₀ > 14 m/s
Sea State 3	14	16	0.35 for V ₀ < 14 m/s, 0.7 for V ₀ > 14 m/s

Table 4 Sea State conditions used in the HAWC2 simulations

The structural setting of the FVAWT in HAWC2 was performed with the controller implemented, middle stiff blades, flexible tower and hydrodynamic drag coefficient Cd=1 as described in the “Detailed Load Analysis of the baseline 5MW DeepWind Concept”; a similar setting was implemented in the FHAWT.

From Figure 26, it is observed that power curve for the FVAWT experiences a high standard deviation of the power above 10m/s compared with the more stable fluctuations on the FHAWT. It is also important to highlight that on one hand the FVAWT is a stall regulated wind turbine and in the other hand the FHAWT is variable speed and pitch regulated wind turbine; therefore, the mean power is not kept constant for the FVAWT compared to the FHAWT due to this different control approach.

In addition, by increasing the sea state level, the waves amplitude become larger and these induce damped blade relative velocities variation in the rotor blades of the FVAWT, this originates a reduction in the power std. deviation of the FVAWT when the sea state increases. Simultaneously, the FVAWT power output trends to increase at this sea state variation due to the rotor blades work under higher relative velocities.

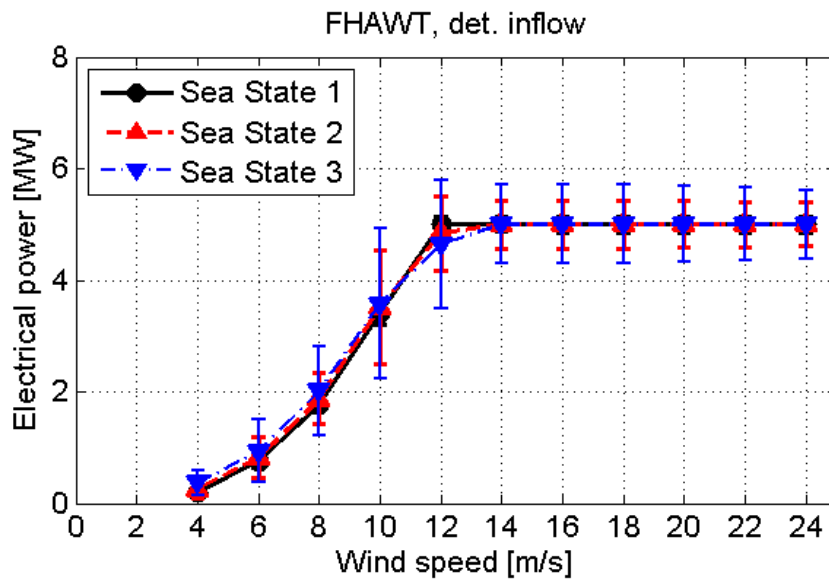
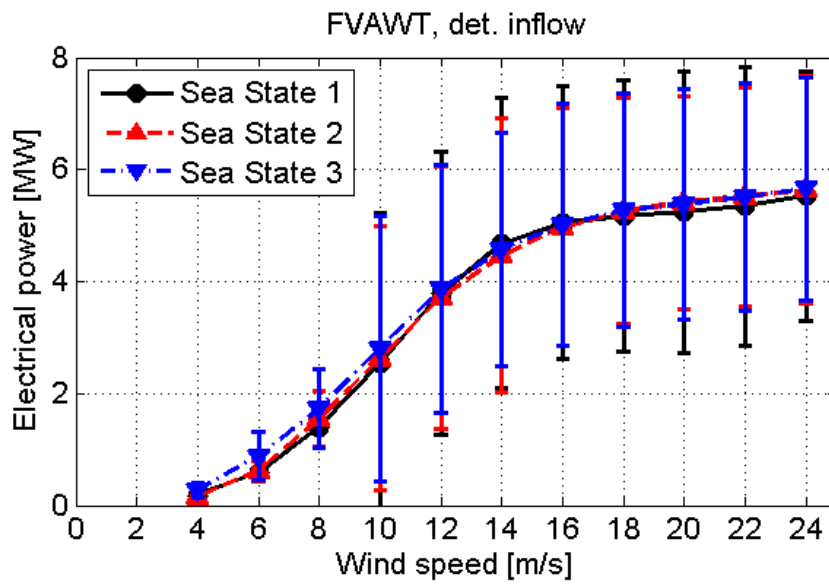


Figure 27 Power curves for the FVAWT Deepwind 5MW and the FHAWT NREL 5MW with deterministic inflow

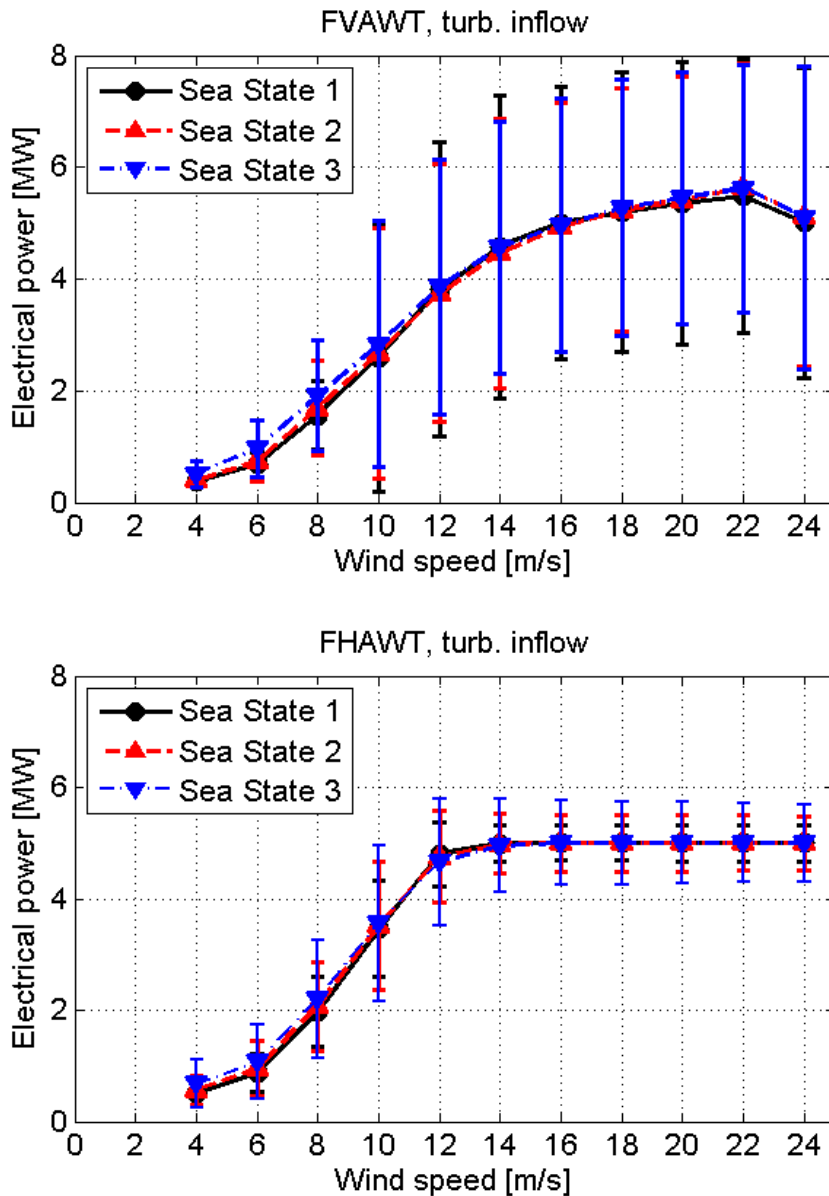


Figure 28 Power curves for the FVAWT Deepwind 5MW and the FAWT NREL 5MW with turbulent inflow

By comparing Figure 26 and Figure 27, it is concluded that the mean power curves for both FVAWT and FAWT are largely unaffected by the turbulent inflow against the deterministic inflow. However, for the turbulent case there is a drop in power starting at wind speeds above 22m/s for FVAWT. An explanation for this can be that because of the high turbulence, the local angles of attack in the rotor blades change largely, and this produce a drop in the lift forces and a fall in the output torque of the FVAWT. Also, the FVAWT turbine controller implements storm control above wind speeds of 23 m/s that gradually reduces the turbine rotational speed (Deliverable 4.2) that would result in a slight drop in generated power.

3.2 Annual Energy Production (AEP)

Based on the results of the previous section, the performance comparison of the FVAWT and FFAWT was performed with the Sea State Level 2 and for deterministic and turbulent inflow due to the smaller power standard deviation for high wind speeds in these operation cases.

For the analysis of the Annual Energy Production (AEP) a Wind Turbine class IIB was selected with an average wind speed at hub height of 8.50 m/s. A Rayleigh wind speed probability distribution was implemented using a scale factor $C=9.59$ and a shape factor $k=2$.

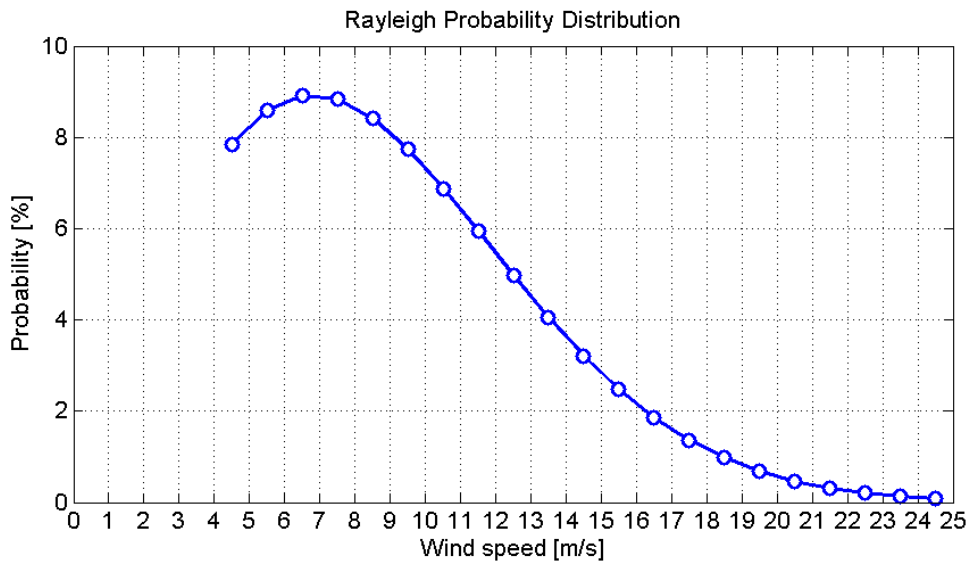


Figure 29 Rayleigh Probability distribution

Table 5 Annual Energy Production Comparison

Annual Energy Production AEP [GWh]			
FVAWT		FFAWT	
Det. Inflow	Turb. Inflow	Det inflow	Turb. inflow
20.133	20.665	22.407	22.934

As expected the FFAWT has a higher AEP for the both cases analyzed (deterministic and turbulent inflow). This is due to the fact that the FFAWT has a lower rated wind speed ($V_{rated}=12\text{m/s}$) compared with the FVAWT ($V_{rated}=14\text{m/s}$). Moreover, because the annual average wind speed for this site is assumed to be 8.5m/s, the probability of wind speeds is mostly concentrated below the FVAWT rated wind speed; therefore, this adds to the discrepancy between the FFAWT and FVAWT.

For the next sections, the structural model for the FVAWT was simulated in HAWC2 without the controller implementation, with 200% stiff blades and stiff tower; moreover, the FVAWT was implemented with similar structural characteristics but with its controller implemented normally. The FVAWT and FVAWT simulations were performed again for wind speeds (deterministic inflow only) in the range from 4 to 24 m/s with a wind step of 2m/s and for 1000s for each wind speed. For the FVAWT the controller was disabled due to high load fluctuations obtained at the moment to post process the HAWC2 results. By implementing a rotor fixed rpm at each wind speed (average rpm for each wind speed with the controller implemented), reasonable results were acquired and these were used to compare them with the FVAWT result values.

The global coordinate system was used for the HAWC2 outputs for both wind turbine models, the wind, waves and current are in the positive Y axis direction, pointing perpendicular to the rotor plane in the case of the FVAWT, X direction is in the FVAWT rotor plane and Z direction is pointing positive to the sea bottom in both cases. The origin of these global coordinate systems is in the floater bottom respectively.

For the relative movement and rotation of the wind turbines, it is important to mention which movement refers to each axis, therefore:

- Surge: refers along Y direction
- Sway: refers along X direction
- Heave: refers along Z direction
- Tilt: refers around X axis
- Roll: refers around Y axis
- Yaw: refers around Z axis

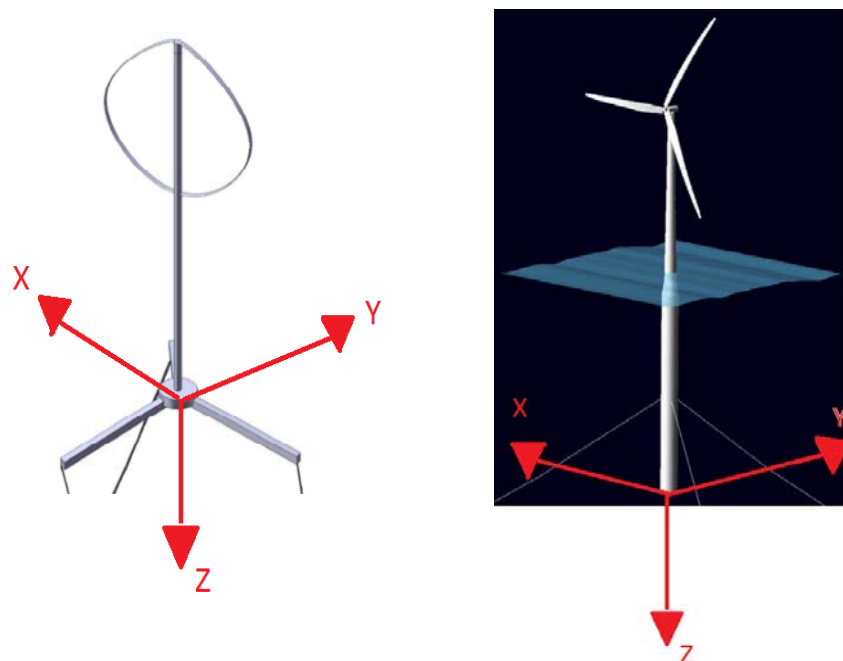


Figure 30. Global coordinate system for the FVAWT and the FVAWT

Illustration by: Luca Vita, Risø DTU, "Offshore Floating Vertical Axis Wind Turbines with Rotating Platform"
 J. Jonkman, NREL, "Definition of the Floating System for Phase IV of OC3"

3.3 Inclination angles of the floating wind turbines (tilt, roll and yaw)

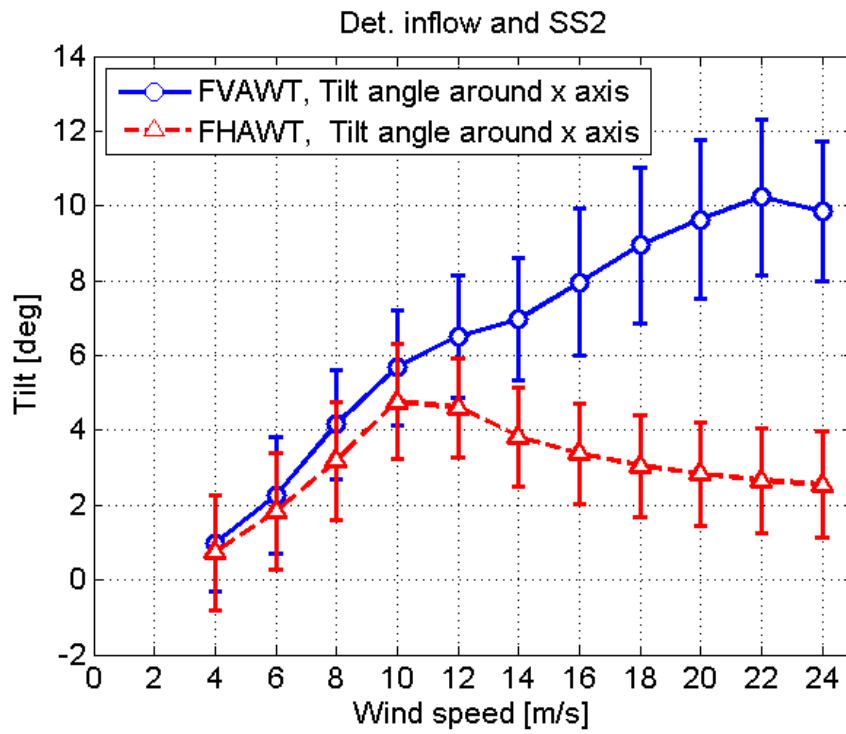


Figure 31 Tilt angle for the FVAWT and FHAWT, deterministic inflow, Sea State 2

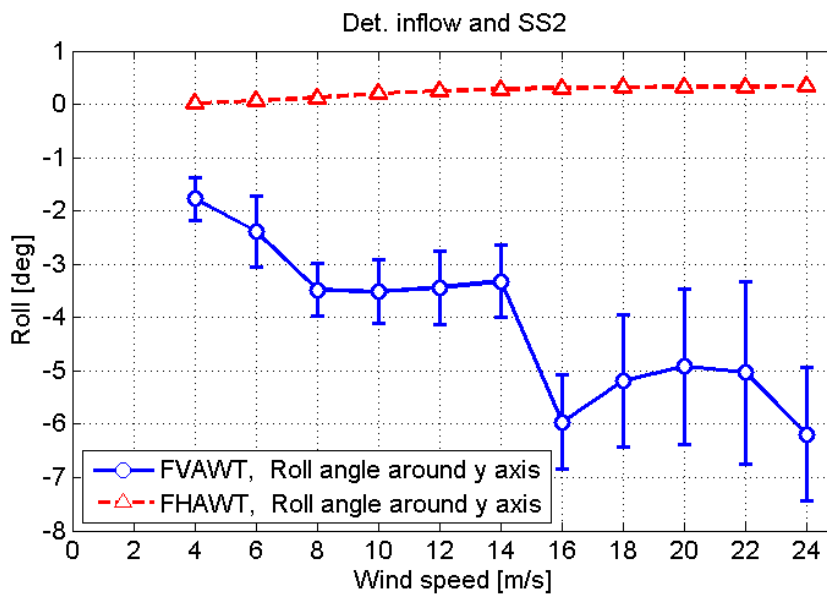


Figure 32 Roll angle for the FVAWT and FHAWT, deterministic inflow, Sea State 2

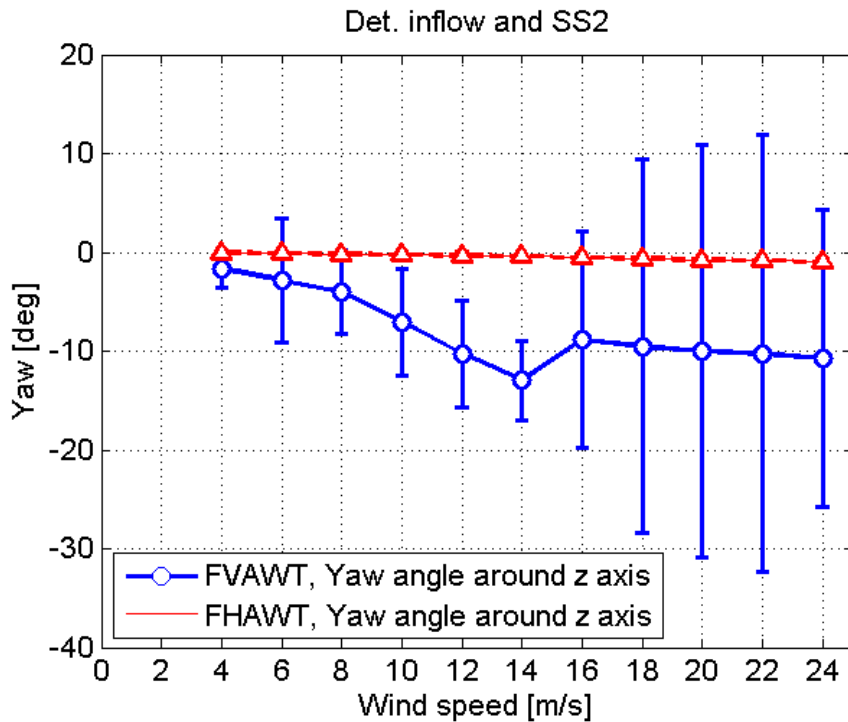


Figure 33 Yaw angle for the FVAWT and FHAWT, deterministic inflow, Sea State 2

From the Tilt angle plot, it is observed that the inclination angle follows exactly the same trend of the thrust curve of each wind turbine. For the FHAWT, this angle curve decreases when the wind speed is close to its rated value because of the blade pitching starts working; however, for the FVAWT this inclination increases permanently because of its fixed blades. This DOF is heavily damped by the fore-aft aerodynamic damping of the rotor in both cases.

For the Roll angle plot, it is clearly observed the Magnus effect, producing a negative inclination angle due to the rotation of the floater below sea level for the FVAWT. In the other hand for the FHAWT the value is close to zero because wind and waves are not affecting the structure in this DOF.

In the Yaw angle plot, for the FVAWT case, the angle of the rotation of the last point of the generator housing (attached to the mooring lines) is plotted; this is because for this wind turbine, the generator housing is the only part submerged that is restricted (partially) by the mooring lines in this DOF. This yaw angle for the FVAWT follows the trend of the torque curve of the wind turbine. For the FHAWT this angle is expected to be close to zero because there is no torque in this direction.

3.4 Position of the floater at tower bottom (sway, surge and heave)

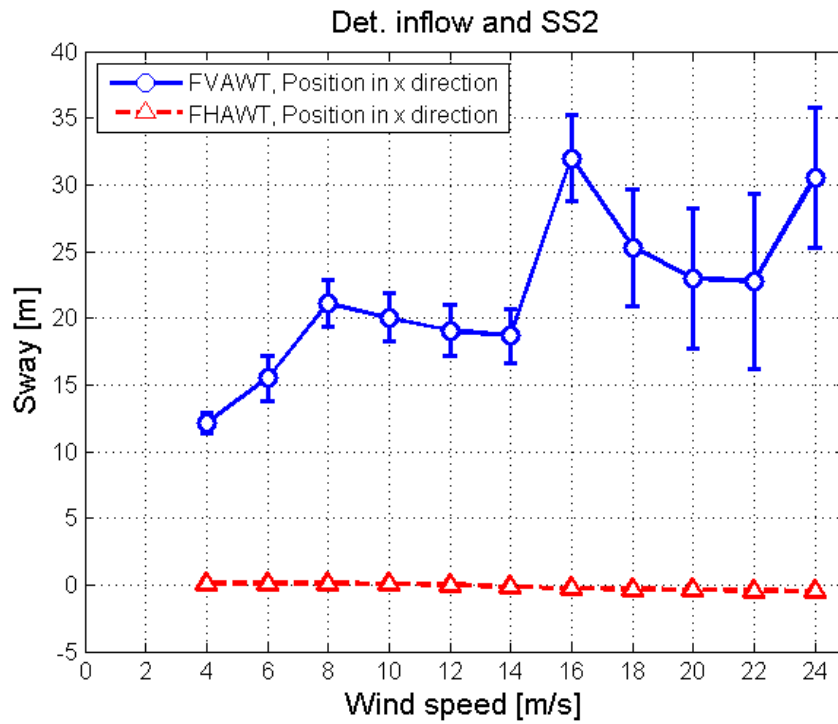


Figure 34 Sway position for the FVAWT and FHAWT, deterministic inflow, Sea State 2

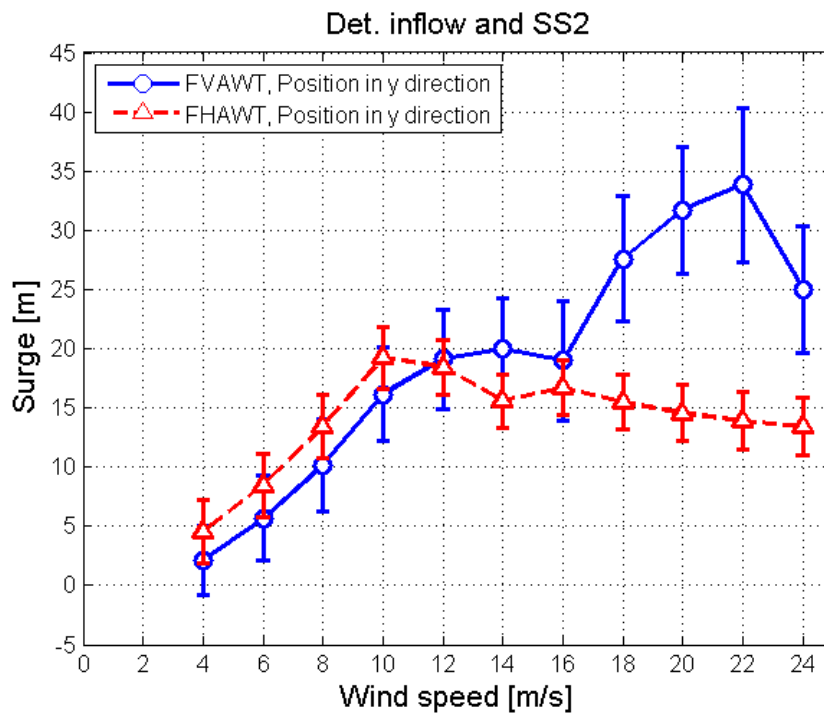


Figure 35 Surge position for the FVAWT and FHAWT, deterministic inflow, Sea State 2

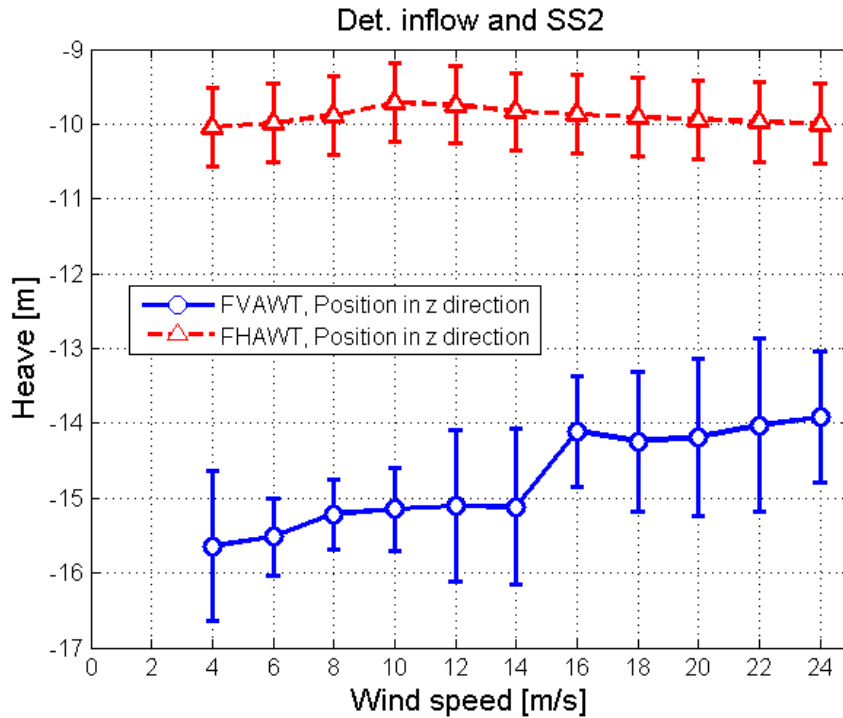


Figure 36 Heave position for the FVAWT and FHAWT, deterministic inflow, Sea State 2

For the Sway position of the FHAWT tower bottom, it is expected to observe a small variation in this position, with a mean value of zero because there are no relevant loads applied along the rotor plane of the wind turbine, that is not the case for FVAWT where the Magnus effect is present with a maximum displacement of more than 30m for 16m/s wind speed.

The Surge position has the same thrust force curve trend for both cases, for the FHAWT, it starts to decrease when the rated wind speed is reached due to the blade pitching and for the FVAWT this increases steadily.

The Heave plot must be observed carefully because the negative value means that the direction of the position is pointing up, referring to the mean sea level. For the FVAWT the tower bottom in steady sea water stays on 16m above sea level and for the FHAWT this position stays on 10m above sea level. It can be observed that for FVAWT the tower bottom tends to sink when the wind speed increases due to the Magnus effect, this originates an inclination of the tower and some aerodynamic loads point downwards. For the FHAWT the maximum sinking is close to V_{rated} due to the at this point the wind turbine withstands the higher thrust loads and the structure has a high tilt inclination.

3.5 Forces at tower bottom

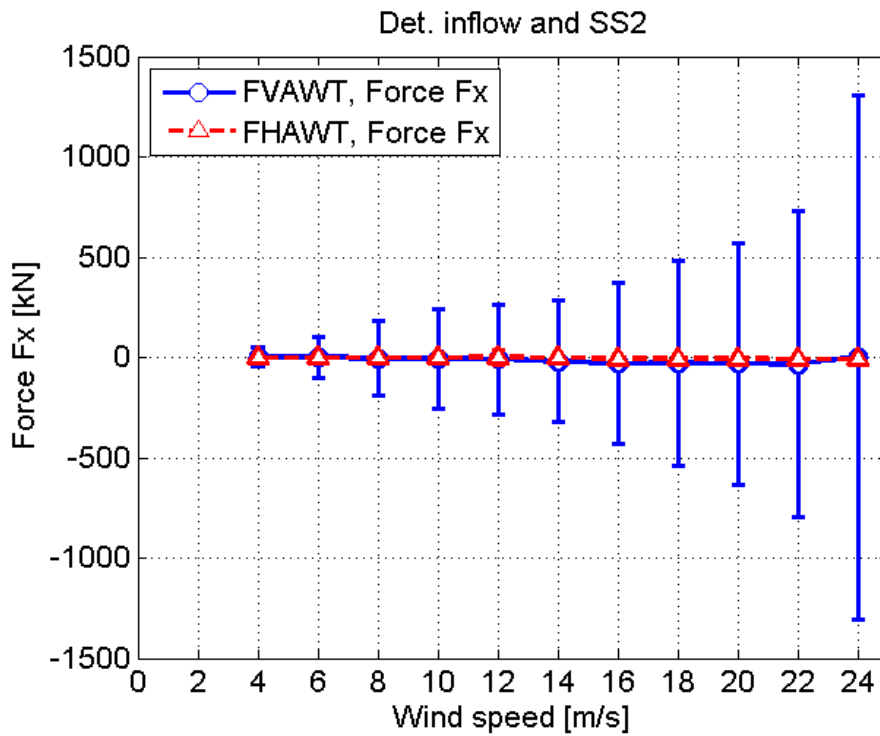


Figure 37 Shear force F_x at tower bottom for the FVAWT and FHAWT, deterministic inflow, Sea State 2

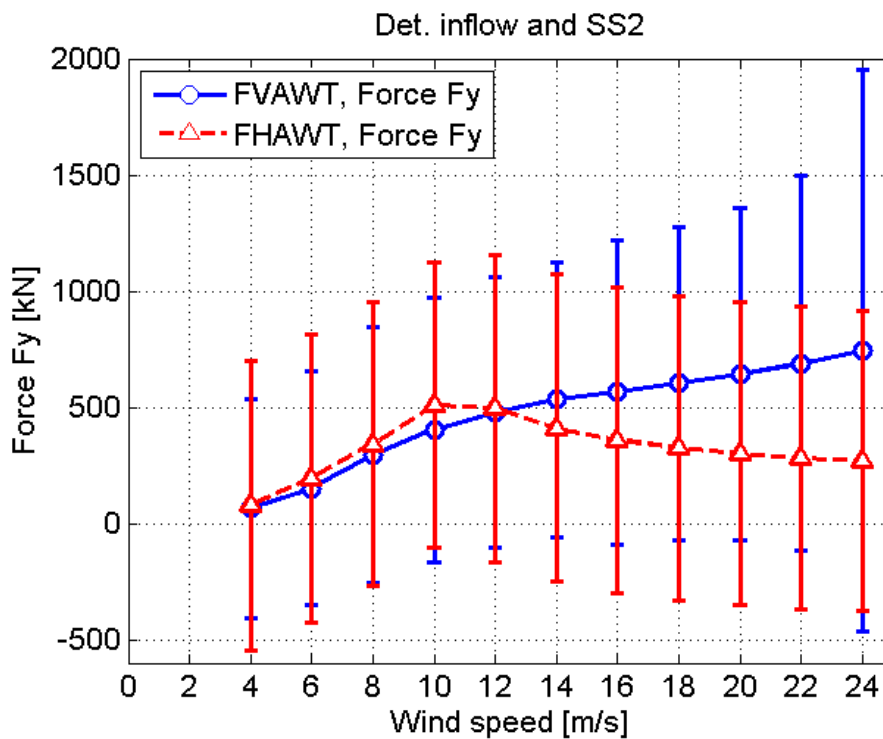


Figure 38 Shear force F_y at tower bottom for the FVAWT and FHAWT, deterministic inflow, Sea State 2

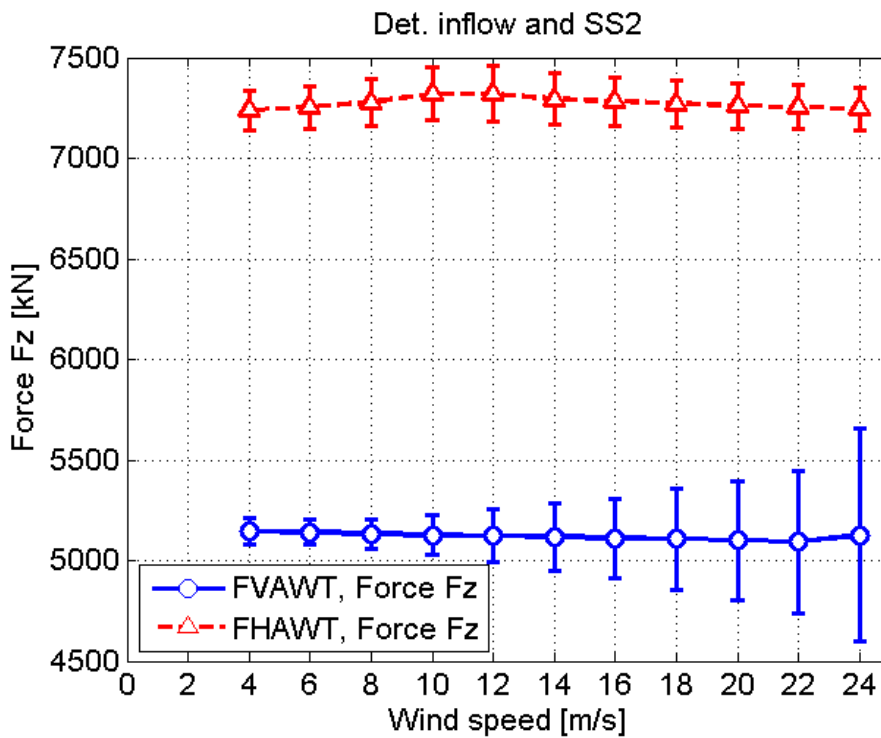


Figure 39 Force Fz at tower bottom for the FVAWT and FHAWT, deterministic inflow, Sea State 2

Regarding the shear forces in the tower bottom, these again refer to the global coordinate system and follow largely the global aerodynamic forces trends for the FVAWT and the FHAWT. In the rotor plane direction (F_x), a mean value is observed for both wind turbine models with high fluctuations for the FVAWT due to the rotor blades loads changing over one revolution. For the forces perpendicular to the FHAWT rotor plane (F_y), again the trend follows the thrust curve for both models.

It is relevant point out that for the F_z forces, compression values are observed, the mean values for both wind turbine models stay constant and the highest values are always for FHAWT; this is coherent because the mass of the FHAWT is concentrated in the nacelle (above the tower bottom); on the other hand for FVAWT the mass is concentrated at the bottom of the floater (below the tower bottom).

3.6 Bending moments at tower bottom

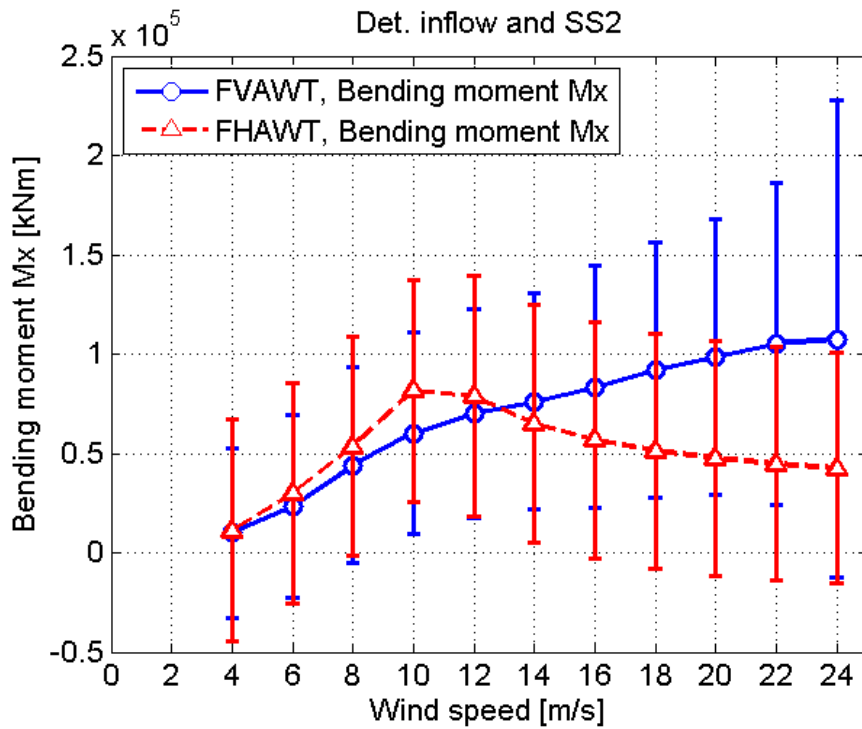


Figure 40 Bending Moment Mx at tower bottom for the FVAWT and FHAWT, deterministic inflow, Sea State 2

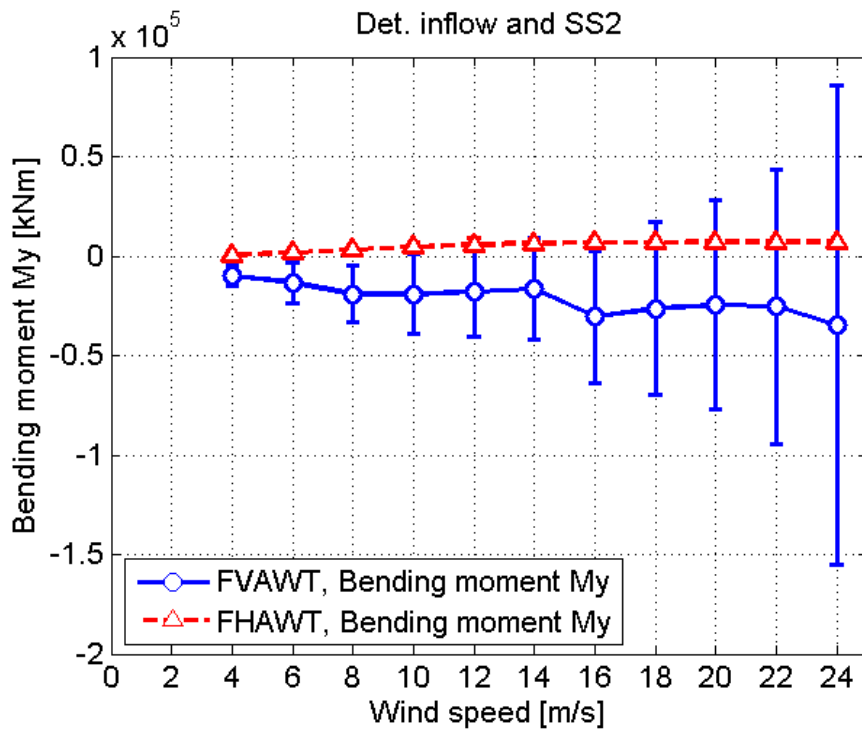


Figure 41 Bending Moment My at tower bottom for the FVAWT and FHAWT, deterministic inflow, Sea State 2

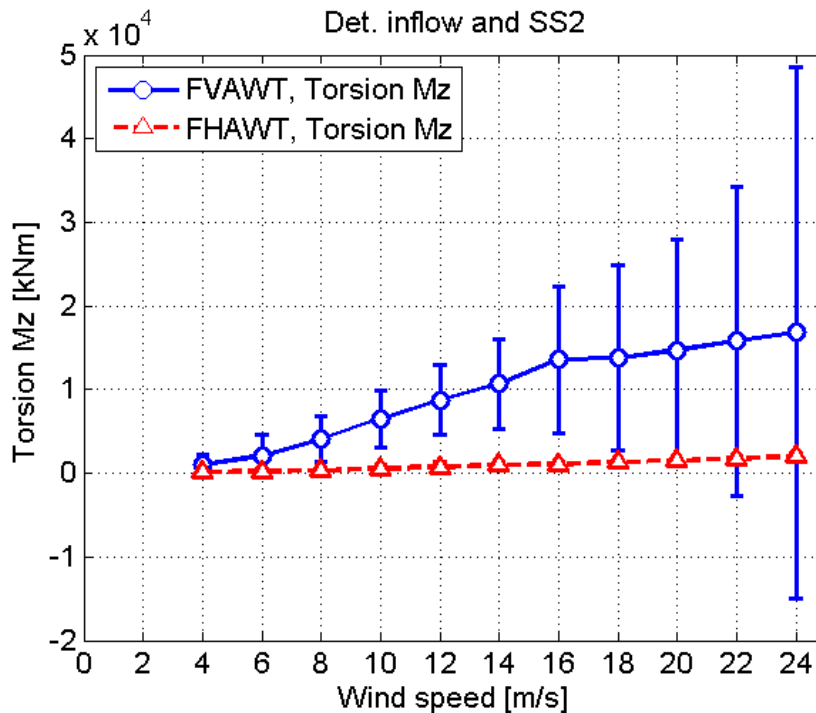


Figure 42 Torsion Mz at tower bottom for the FVAWT and FHAWT, deterministic inflow, Sea State 2

From the bending moment plots at the tower bottom it can be observed that for the for-after Mx bending moment, the magnitudes are comparable with each other for both wind turbine models, but the maximum values are reached at different wind speeds, V_{rated} for FHAWT and V_{out} for the FVAWT. This trend was observed for all the cases where the wind turbines were affected in the direction of the wind, wave and current loads (same direction of three effects).

For the bending moment on the My direction, it is observed clearly the Magnus affect again on the FVAWT, this force incline the tower and impose a permanent moment in the tower bottom that increases with the wind speed. For the FHAWT the mean value remains close to zero as expected because of the absence of relevant external loads that would produce moments in this direction.

In the Torsional plot, the torque at the tower bottom of the FVAWT is observed; high standard deviations for wind speeds above V_{rated} appeared because these simulations were performed in HAWC2 without the controller implementation and with fix rpms.

3.7 Bending moments from the blade root (bottom) to the blade root (top)

The moments on the blade root were calculated using the local coordinate system of the blade; that reflects, that the X axis is on the chord line of the blade section pointing the leading edge, the Y axis is point the suction side of the blade section (this changes of direction depending if it refers to bottom blade root or top blade root) and the z axis goes along the spanwise direction of the blade, from the blade root to tip for the FHAWT, and from bottom blade root to top blade root for the FVAWT.

This blade coordinate system is well described for the Blade section i,2 in [2]:

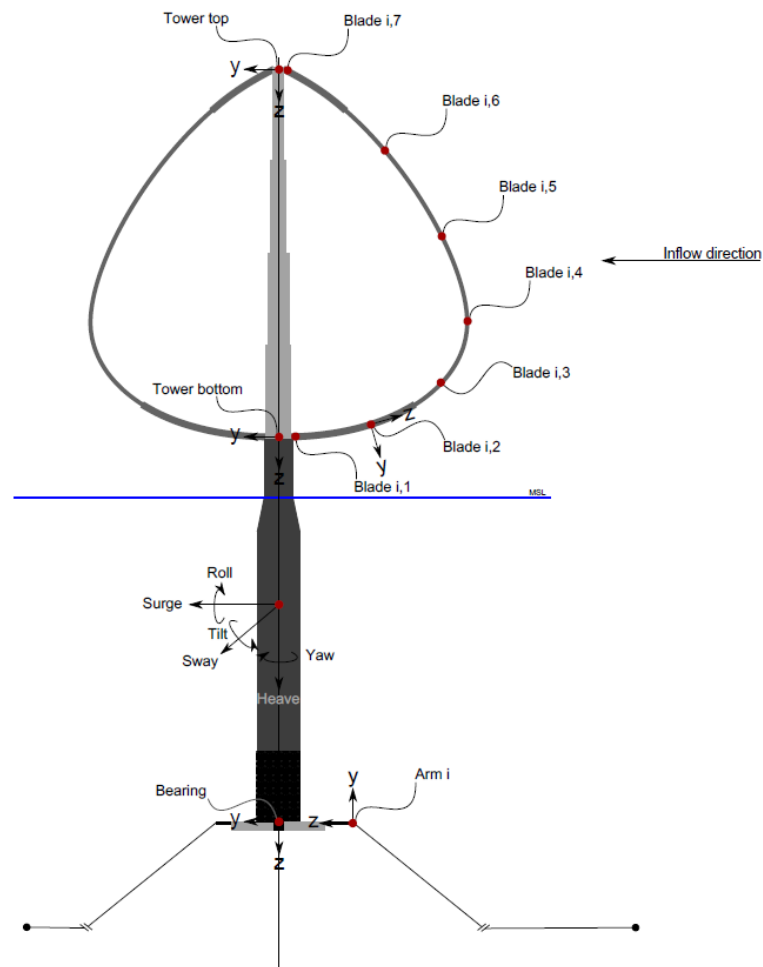


Figure 43 Positions and coordinate systems of the points at which forces, moments and positions

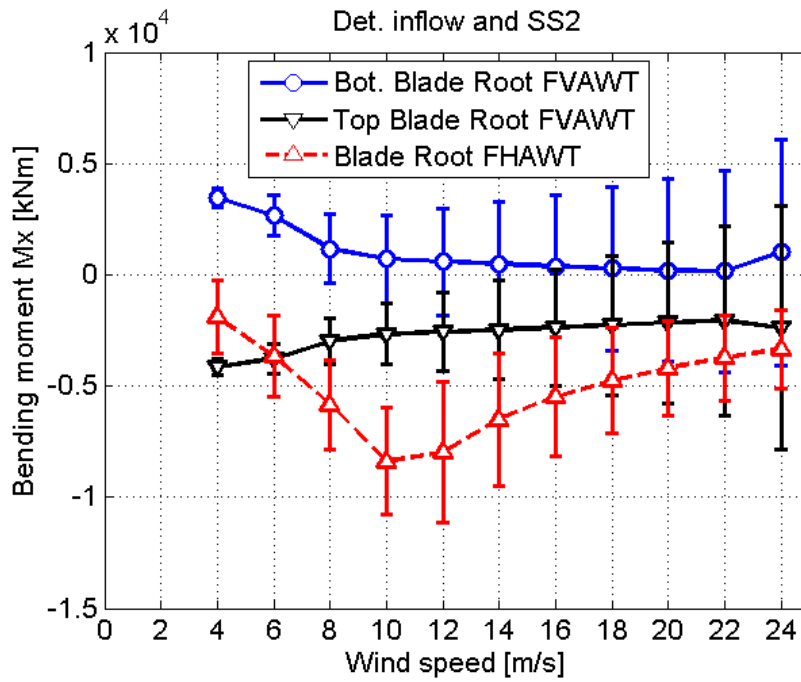


Figure 44 Bend. Moment Mx at the blade roots for the FVAWT and FFAWT, deterministic inflow, Sea State 2

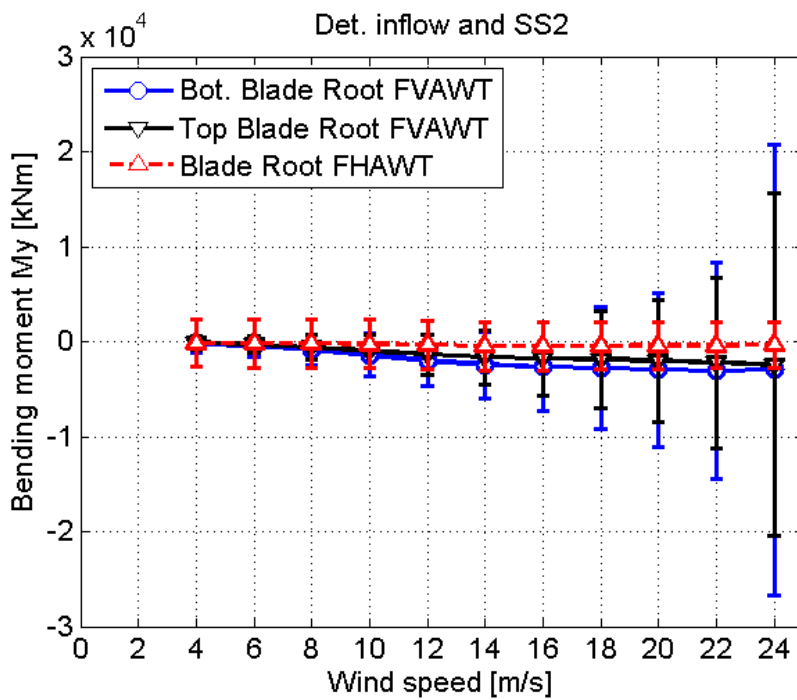


Figure 45 Bend. Moment My at the blade roots for the FVAWT and FFAWT, deterministic inflow, Sea State 2

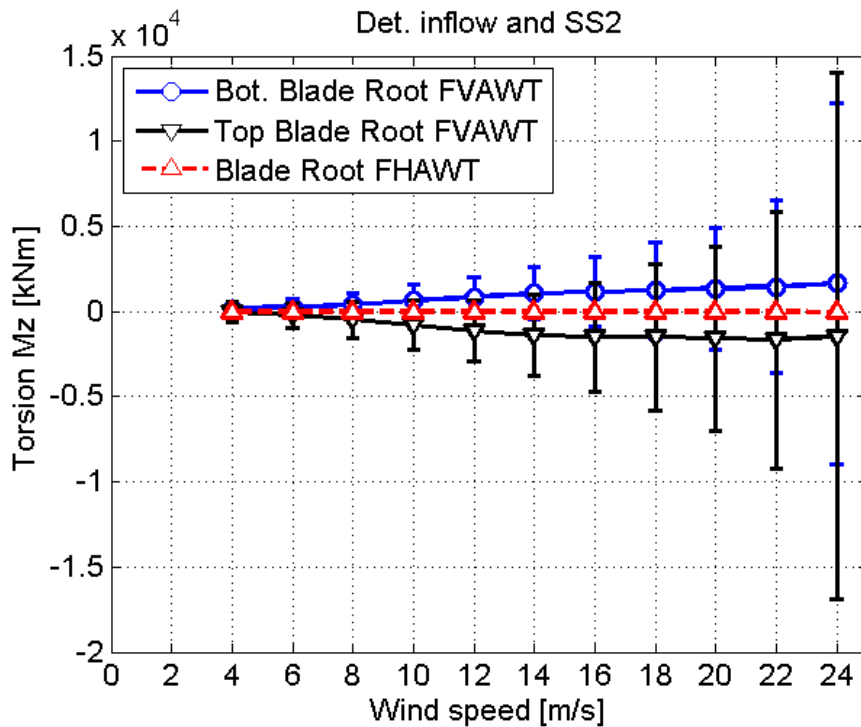


Figure 46 Torsion Mz at the blade roots for the FVAWT and FHAWT, deterministic inflow, Sea State 2

For the Flapwise direction bending moments on the blade roots, it can be concluded that FVAWT blade root moments std. deviations are comparable in magnitude to the ones experienced by FHAWT. Indeed, the mean values of the FVAWT blade roots are more constant over the operating range (even reducing when increasing to rated wind speed); this is most probably as the blade mass counteracted partially by centrifugal forces.

It is also interesting to highlight that for the flapwise bending moments have maximum values at different wind speeds, for FHAWT occurred around rated wind speed but for the FVAWT occurred at low wind speeds (cut in wind speed). This will have a negative impact on the fatigue analysis considering a wind speed probability distribution with a low average wind speed site.

For the edgewise moments and torsions on the blade root for both wind turbine models, the magnitudes tend to increase along the operational range and the standard deviation also, the high fluctuations are presumably because of the no implantation of the controller once again.

3.8 Concluding Remarks

Overall the FVAWT experiences similar loads to the FHAWT, but the load predictions are heavily dependent on the implemented numerical model that currently is limited from a structural standpoint. Also, the predicted AEP's of the FHAWT and FVAWT are very similar, despite that the site conditions favor the FHAWT lower rated wind speed and hub height.

The two systems experience maximum loads at different operating conditions, with the FHAWT experiences maximum loads around the rated wind speed (12m/s) and the FVAWT experiencing maximum loads at the cut-off wind speed (25m/s).

As the FVAWT experiences the Magnus effect on the submerged rotating spar, the system experiences significantly larger lateral (sway, roll) displacements than the FHAWT that only has significant thrust loads.

An important aspect is that at the tower-floater connection, the FVAWT experiences significantly lower vertical forces than the FHAWT as the mass of the VAWT turbine is distributed above (rotor and turbine) and below (generator) this connection point.

In summary, the FVAWT concept is comparable to the FHAWT design considering the model limitations established above, and further work is warranted to bring this concept forward to be one of the most promising floating wind energy devices.

References

- [1.] Schmidt Paulsen Uwe, Schløer Signe, Larsén Xiaoli, Hahmann Andrea, Larsen Søren, Larsen Torben, Troels, Pedersen Ole Svenstrup (DHI) The DeepWind Concept D8.1 Specifications/ Prerequisites for DeepWind DTU-Wind Energy-E-0044(EN) July 2014
- [2.] Verelst David, Kragh. K. Madsen Helge Aa. , Belloni, F. Detailed Load Analysis of the baseline 5MW DeepWind Concept. DTU Wind Energy-E-0057,DTU 2014
- [3.] Schmidt Paulsen Uwe S., Madsen Helge Aa,Kragh Knud,Nielsen, P.H.,Baran I.Rietchie E.,Leban Krisztina M.,Svendsen Harald,Berthelsen Petter A.,van Bussel Gerard J.W.,Ferreira, Carlos S.,Chrysochoidis-Antsos Nichos The 5 MW DeepWind floating offshore vertical wind turbine concept design - status and perspective part of: Proceedings - EWEA 2014, 2014, European Wind Energy Association (EWEA), Presented at: European Wind Energy Conference & Exhibition 2014, 2014, Barcelona Article in proceedings (Peer reviewed)
- [4.] Schmidt Paulsen Uwe ; Aagaard Madsen Helge ; Nielsen Per Hørlyk ; Kragh, Knud Abildgaard ; Baran, Ismet ; Hattel, Jesper Henri ; Ritchie, Ewen ; Leban, Krisztina ; Svenden, Harald ; Berthelsen, Petter A DeepWind.From idea to 5 MW concept. Presented at: EERA DeepWind 2014 - 11th Deep Sea Offshore Wind R&D Conference, 2014, Trondheim
- [5.] Baran I, Tutum CC, Hattel JH. The internal stress evaluation of the pultruded blades for a Darrieus wind turbine. Key Eng. Mat. 2013; 554-557: 2127-2137.
- [6.] Leban Krisztina, Ritchie, Ewen,. Design of generator system DeepWind report 6 pp 2012. Deliverable D3.2 Design of generator system AAU October 2012
- [7.] Leban Krisztina, Ritchie, Ewen, Development tool for generator design. DeepWind report 6 pp 2012. Deliverable D3.1 Development tool for generator design AAU, October 2012
- [8.] Berthelsen Petter Andreas, Fylling Ivar Conceptual design of a floating support structure and mooring system for a vertical axis wind turbine Omae Proceedings of the ASME 2012 31st International Conference on Ocean, Offshore and Arctic Engineering 2012.
- [9.] Berthelsen Petter Andreas Conceptual design of a floating support structure and mooring system for the DeepWind project. D5.2 September 2014.
- [10.] Chrysochoïdis-Antsos Nikolaos The conceptual design of a safety system For the 5MW Deepwind Wind Turbine Master thesis report May 2014, Delft university
- [11.] Paulsen, U.S. Deepwind: Estimation Of Water Friction On Cylinder Parts Along The Perimeter Internal note, DTU 2014 7 pp.
- [12.] ISO/DIS 19901-1 Petroleum and natural gas industries — Specific requirements for offshore structures —Part 1: Metocean design and operating considerations
- [13.] See also ref lists in D3.1-D.4, D3.31,D3.32

Acknowledgements

The DeepWind beneficiaries: DTU(DK), AAU(DK), TUDELFT(NL), TUTRENTO(I), DHI(DK), SINTEF(N), MARINTEK(N), MARIN(NL), NREL(USA), STATOIL(N), VESTAS(DK) and NENUPHAR(F) are acknowledged for their contributions.

The European Commission is acknowledged for supporting the DeepWind project under project number 256769

DTU Wind Energy is a department of the Technical University of Denmark with a unique integration of research, education, innovation and public/private sector consulting in the field of wind energy. Our activities develop new opportunities and technology for the global and Danish exploitation of wind energy. Research focuses on key technical-scientific fields, which are central for the development, innovation and use of wind energy and provides the basis for advanced education at the education.

We have more than 240 staff members of which approximately 60 are PhD students. Research is conducted within nine research programmes organized into three main topics: Wind energy systems, Wind turbine technology and Basics for wind energy.

Technical University of Denmark

Department of Wind Energy
Frederiksborgvej 399
Building 118
4000
Denmark
Phone 46 77 50 85

info@vindenergi.dtu.dk
www.vindenergi.dtu.dk

Roskilde